J. Fluid Mech. (1973), *vol.* 61, *part* 1, *pp.* 129–158
Printed in Great Britain

Waves generated in rotating fluids by travelling forcing effects

By G. V. PRABHAKARA RAO
Department of Mathematics, Indian Institute of Technology, Madras

(Received 23 February 1973)

The two-dimensional wave pattern produced in a homogeneous rotating fluid by a forcing effect oscillating with a frequency σ_0' and travelling with a uniform speed U along a line inclined to the axis of rotation at an arbitrary angle α is studied following Lighthill's technique. It is shown how the far field changes with α and σ_0'.

For all $\sigma_0' < 2\Omega$, except for $\sigma_0' = 2\Omega \sin\alpha$ (Ω being the angular velocity of the fluid), the forcing effect excites two systems of waves. When $\sigma_0' \to 2\Omega \sin\alpha$ one of these systems spreads out, influencing the upstream side while the other shrinks in the downstream direction. This upstream influence is to the left or to the right of the line of motion of the forcing effect (the forcing line) according as $\sigma_0' - 2\Omega \sin\alpha \lesseqgtr 0$ and increases as $\sigma_0' - 2\Omega \sin\alpha$ decreases. For $\sigma_0' > 2\Omega$ there is only a single system propagating downstream. As α varies these systems undergo a kind of rotation retaining the main features. $\alpha \neq 0$ or $\frac{1}{2}\pi$ makes the pattern asymmetric about the forcing line while a non-zero σ_0' splits the steady-case identical wave systems into two, which are otherwise coincident.

When $\sigma_0' = 2\Omega \sin\alpha$ the forcing effect excites straight unattenuated waves of fixed frequency travelling both ahead and behind in a 'column' parallel to the forcing line and enclosing it. Also there are two other systems, which propagate without penetrating into an upstream wedge. It is shown that this 'column' is the counterpart of the 'Taylor column'.

1. Introduction

In geophysical fluid dynamics, which includes the study of rotating fluids and stratified fluids, many types of wave systems are possible and it is desirable to know how they can be excited by different types of forcing effects. With this motivation, following a technique developed by Lighthill (1960), several problems under different conditions have been studied by Nigam & Nigam (1962), Lighthill (1967), Mowbray & Rarity (1967), Stevenson (1969), Subba Rao & Prabhakara Rao (1971), and others. This paper deals with the excitation of such waves by a forcing effect travelling in an arbitrary direction with a uniform velocity U and oscillating with a frequency σ_0' in a homogeneous rotating fluid.

Plane inertial waves in a rotating fluid are dispersive, anisotropic and are circularly polarized (cf. Greenspan 1968, p. 187). So the wave patterns produced by forcing effects travelling in different directions are not in general the same.

The pattern depends only on the azimuthal angle of the line of motion of the forcing effect (the 'forcing line' for short) but not on the meridional angle. This urges one to explore the situation in which the forcing effect travels in an arbitrary direction. The complications encountered in solving problems of this type are numerous and often intractable. In view of this only a two-dimensional forcing effect (for which everything is independent of the distance y in a direction fixed in a rotating frame of reference and perpendicular to the axis of rotation) is considered and it is hoped that this will throw some light on more complicated three-dimensional problems. These forcing effects could be any type of disturbing agencies like a horizontal cylinder moving parallel to itself and oscillating or a combination of line sources and sinks, etc. No attempt has been made so far to determine the wave pattern excited in rotating fluids by a two-dimensional forcing effect travelling in an arbitrary direction. Nevertheless, from the existing literature it is possible to derive the main features of the pattern in some special cases using certain well-established analogies. All such results are recalled here first and the cases not covered by them are studied in detail in the text. It is also indicated in the text how the several patterns for arbitrary direction correspond to these special cases.

The excitation of waves in a homogeneous rotating fluid by steady forcing effects ($\sigma_0' = 0$) travelling along the axis of rotation and the wave pattern have been investigated by Lighthill (1967) and the corresponding oscillatory problem has been studied by Nigam & Nigam (1962). Not only do these problems give an idea of the various wave systems generated but also they help one to envisage some of the interesting phenomena in rotating fluids. In particular, Lighthill (1967) explains most clearly and in a simple manner, in terms of plane inertial waves, the formation of the 'Taylor column', its structure and the presence of spherical waves downstream. On the other hand, Nigam & Nigam (1962) explain how new systems of waves evolve with the oscillations of the forcing effect and how the frequency makes it possible to influence the upstream side by exciting waves which propagate ahead of the forcing effect. The similarity between axisymmetric flows and planar ones in a rotating fluid (cf. Bretherton 1967) implies that a two-dimensional forcing effect travelling along the axis of rotation also generates similar wave pattern. Hence the entire two-dimensional pattern is also symmetric about the forcing line. The steady forcing effect excites cylindrical waves of uniform wavelength $\pi U/\Omega$, Ω being the angular velocity of the fluid, propagating in all directions on the downstream side. Also, a two-dimensional analogue of the 'Taylor column' (hereafter denoted by $\mathscr{T}$) extending indefinitely both ahead and behind also appears. The upstream part of $\mathscr{T}$ is filled with straight unattenuated plane waves travelling parallel to the axis of rotation with wavelengths greater than $\pi U/\Omega$ (the low-pass filter) and the downstream part of $\mathscr{T}$ is composed of similar waves with no restriction on their wavelengths. When the forcing effects oscillate with a frequency $\sigma_0' < 2\Omega$ the upstream part of $\mathscr{T}$ and a part of the downstream cylindrical waves combine into a new system propagating in all directions but not penetrating into an upstream wedge of semi-angle $\sin^{-1}(\sigma_0'/2\Omega)$ with parabola-like wave crests. The rest of the waves combine into another system and propagate downstream either in a continua-

tion of the upstream wedge or a wedge determined by the cusp loci of their wave crests (cf. figure 7). The wave crests have the shape of a flared skirt with an inverted curved triangle for its head. As σ_0' increases to 2Ω the upstream wedge tends to a plane perpendicular to the forcing line while the wedge formed by the cusp loci shrinks. So the system influencing the upstream side is gradually compressed towards the downstream side and disappears completely when $\sigma_0' = 2\Omega$. The flared-skirt pattern spreads out to give propagation in all directions below the forcing effect while the curved triangular head shrinks. For $\sigma_0' > 2\Omega$ the flared-skirt pattern becomes folded upon itself, forming another bigger curved triangle, and all the waves propagate downstream, confining themselves to the wedge determined by the loci of the cusped vertices of the bigger triangle. If σ_0' increases further this system simply shrinks.

The analogy between the motion in a vertical plane in a Boussinesq stratified fluid and the planar motion in a rotating fluid (Veronis 1970) provides an immediate translation of the description from stratified systems in terms of internal waves to rotating systems in terms of inertial waves. With special reference to the type of problems considered in this paper, this analogy means that the wave pattern excited in a stratified fluid by a forcing effect travelling at an angle α to the vertical, and the wave pattern excited in a homogeneous rotating fluid by a forcing effect travelling at an angle $\frac{1}{2}\pi - \alpha$ to the axis of rotation are mirror images of each other in the forcing line provided that the corresponding parameters in both the fluid systems have the same values and the forcing effect in one fluid system is the reflexion of the other in the forcing line.

When a forcing effect travels with a uniform velocity in an arbitrary direction in a homogeneous rotating fluid this analogy enables one to derive all the important features of the wave pattern directly from Rarity (1967), who studied the two-dimensional internal wave pattern produced by a steady ($\sigma_0' = 0$) disturbance moving with a uniform velocity along a line of arbitrary inclination. For a given inclination α of the forcing effect, the wavenumber curves and the lines of constant phase associated with a rotating fluid are respectively reflexions, in the line $K_2 = 0$ and $Y = 0$, of the figures given by Rarity (1967) for an inclination $\frac{1}{2}\pi - \alpha$. The pattern consists of a single system of waves (which is actually a superposition of two identical wave systems) propagating in all directions which are to the left of a line passing through the centre of the forcing effect and inclined at an angle α to the forcing line, where $0 < \alpha < \frac{1}{2}\pi$ and α is measured counterclockwise. The crests and the lines of constant phase are cusped curves with their arms asymptotic to the above-mentioned boundary line. The cusp locus is to the right of the forcing line, in the fourth quadrant. There is a caustic along the downstream part of the forcing line and the crests touch the downstream part of the forcing line on the right. These crests travel in the same direction as the forcing effect with phase velocities less than U, the speed of the forcing effect, and the points with horizontal tangents have maximum phase velocity U. As α increases the boundary line and the disturbed region below it rotate about the forcing effect in the counterclockwise sense. The wave crests also rotate about the caustic points in the same sense as the boundary line and tend to become symmetric about the downstream part of the forcing line

and finally take on the 'flared-skirt' pattern when $\alpha = \frac{1}{2}\pi$. As α decreases the boundary line rotates towards the forcing line, thereby influencing larger and larger areas in the upstream side, which is to the left of the forcing line, in the second quadrant. But the situation in the fourth quadrant is different. When α decreases below 19°, the cusp locus which turns away from the downstream part of the forcing line crosses the boundary line (cf. figure 7) and tends to occupy the entire fourth quadrant as $\alpha \to 0$. So as α decreases the disturbed region in the fourth quadrant spreads out or shrinks according as $\alpha \lesseqgtr 19°$. The upper arm of the crest curves, becoming the shape of a walking stick while the lower arm straightens and becomes parallel to the downstream part of the forcing line. When α is sufficiently small the disturbance is found almost everywhere except in the first quadrant. Finally in the limit $\alpha = 0$ this system splits into two parts as in Lighthill (1967).

Axisymmetric internal wave patterns generated by an oscillating body travelling vertically upwards have been studied both theoretically and experimentally by Stevenson (1969). Again using the above analogies the wave pattern due to a two-dimensional forcing effect oscillating with a frequency σ_0' and travelling perpendicular to the axis of rotation with constant velocity in a homogeneous rotating fluid could be derived from Stevenson (1969). Here the wave pattern (and the wavenumber curve) are symmetric about the forcing line and because of this the wavenumber curves and the lines of constant phase for the rotating case are similar to those in the figures given in Stevenson (1969). For $0 < \sigma_0' < 2\Omega$ the wavenumber curve consists of two parabola-like curves passing through the origin and $(0, -\sigma_0'/U)$. The waves associated with the wavenumber curve above the origin propagate downstream, confining themselves to a wedge of semi-angle $\tan^{-1}\{(\sigma_0'/U)\,(4\Omega^2 - \sigma_0'^2)^{\frac{1}{2}}\}$ with flared-skirt crests. The waves associated with the rest of the wavenumber curve propagate in all directions without penetrating into the image of the above wedge in the origin with ω-shaped crests. As $\sigma_0' \to 2\Omega$ the ω-shaped system spreads and propagates in all directions while the flared-skirt system shrinks and becomes a family of straight unattenuated waves propagating downstream parallel to the downstream part of the forcing line. When $\sigma_0' > 2\Omega$, the wavenumber curve becomes a x-shaped curve and the ω-shaped system folds back on itself and propagates only downstream in a wedge with kite-shaped crests. This system gradually shrinks as σ_0' increases further.

The forcing effects travelling in various directions and the patterns generated by them exhibit certain symmetry properties among themselves which are evident from equation (7) below. A forcing effect travelling at an inclination α to the axis of rotation (or the vertical, if the fluid is stratified) and its image in the origin or in the axis of rotation (or the vertical) generate wave patterns which are also images of each other in the origin or the axis of rotation (or the vertical) respectively. For this reason only those forcing effects whose inclination lies between 0 and $\frac{1}{2}\pi$ are considered in this paper. Section 2 gives the governing equations and a formal solution following Lighthill (1967). Section 3 is concerned with the description of the wave pattern for a fixed α and σ_0'. The changes and modifications arising from variations in α and σ_0' are described in § 4. Section 5 is a summary of the salient features of the wave pattern.

2. The governing equations and a formal solution

A large body of inviscid incompressible homogeneous fluid is rotating like a rigid body with a constant angular velocity about an axis Oz and $Oxyz$ is a Cartesian frame rotating with the fluid. The motion in this fluid is generated by a two-dimensional forcing effect of finite extent which is independent of the y co-ordinate, oscillating with a frequency σ_0' and travelling with a constant velocity U at an angle α to Oz, α being measured clockwise. If the motion generated is small then at distances large compared with the dimensions of the forcing effect it constitutes a small perturbation to the rigid rotation and hence takes the form of inertial waves. This perturbation velocity $\mathbf{q}$ in the inertial oscillations satisfies the differential equation

$$\left[\frac{\partial^2}{\partial t^2}\left(\frac{\partial^2}{\partial x^2}+\frac{\partial^2}{\partial z^2}\right)+4\Omega^2\frac{\partial^2}{\partial z^2}\right]\mathbf{q} = \exp\{-i\sigma_0' t'\}\,\mathbf{H}(x-Ut'\sin\alpha, z-Ut'\cos\alpha), \quad (1)$$

where the right-hand side, which vanishes outside a finite region, represents the forcing effect generating the motion (Lighthill 1967).

Consider a new frame of reference $Ox_1y_1z_1$ which is fixed relative to the forcing effect, with Oz_1 along the forcing line and with Oy_1 parallel to Oy. Then the co-ordinates in the two frames are connected by the relations

$$\begin{aligned} x_1 &= \epsilon^{-1}(x\cos\alpha - z\sin\alpha),\\ z_1 &= \epsilon^{-1}(x\sin\alpha + z\cos\alpha) - t,\\ y_1 &= \epsilon^{-1}y, \end{aligned}$$

where $\epsilon = U/2\Omega L$ is the Rossby number, L is a characteristic dimension of the forcing effect, $t = 2\Omega t'$ and all other variables are dimensionless. In this new frame (1) takes the form

$$\left[\left(\frac{\partial}{\partial t}-\frac{\partial}{\partial z_1}\right)^2\left(\frac{\partial^2}{\partial x_1^2}+\frac{\partial^2}{\partial z_1^2}\right)+\left(\cos\alpha\frac{\partial}{\partial z_1}-\sin\alpha\frac{\partial}{\partial x_1}\right)^2\right]\mathbf{q}_1 = \exp\{-i\sigma_0 t\}\,\mathbf{H}(x_1, z_1), \quad (2)$$

where $\mathbf{q}_1$ denotes the velocity vector in the new frame and σ_0 is the dimensionless frequency $\sigma_0'/2\Omega$. A formal solution of (2) is given by

$$\mathbf{q}_1 = \int_{-\infty}^{\infty}\int_{-\infty}^{\infty}\frac{\mathscr{H}(l_1, n_1)}{S(l_1, n_1, \sigma_0, \alpha)}\exp\{-i(-\sigma_0 t + l_1x_1 + n_1z_1)\}\,dl_1\,dn_1, \quad (3)$$

with
$$S(l_1, n_1, \sigma_0, \alpha) = (\sigma_0 + n_1)^2(l_1^2 + n_1^2) - (n_1\cos\alpha - l_1\sin\alpha)^2 \quad (4)$$

and
$$\mathbf{H}(x_1, z_1) = \int_{-\infty}^{\infty}\int_{-\infty}^{\infty}\mathscr{H}(l_1, n_1)\exp\{i(l_1x_1 + n_1z_1)\}\,dl_1\,dn_1, \quad (5)$$

defining the Fourier transform of $\mathbf{H}(x_1, z_1)$.

A method for deriving the asymptotic values of integrals of the type (3) valid at distances large compared with the dimensions of the forcing effect has been given by Lighthill (1960, 1965, 1967). Using this technique the far field could be described in terms of plane inertial waves of the type

$$\exp\{i[-\sigma_0 t + l_1x_1 + n_1z_1]\}. \quad (6)$$

The homogeneous part of the differential equation (2) admits plane-wave solutions (6) provided that

$$S(l_1, n_1, \sigma_0, \alpha) = 0, \tag{7}$$

which represents a curve, the wavenumber curve (hereafter denoted by S), in the l_1, n_1 plane. Since (7) also represents the locus of the singularities of the integrand in (3), each point (l_1, n_1) on S contributes to the value of the integral (3) and a Fourier sum of such solutions gives the total solution. The amplitude of each wave propagating in any particular direction is given by

$$\frac{(2\pi)^{\frac{3}{2}}}{(|\kappa| r_1)^{\frac{1}{2}}} \frac{\mathscr{H}(l_1, n_1)}{|\nabla S(l_1, n_1, \sigma_0, \alpha)|}, \tag{8}$$

where κ is the curvature of the wavenumber curve, $r_1 = |\mathbf{r} - \epsilon \hat{\mathbf{U}} t|$, the distance from the forcing region, and ∇ the gradient operator in the $\mathbf{k}_1 = (l_1, n_1)$ plane. The amplitude of the waves associated with the points at which the curvature of S vanishes, that is the points of inflexion, decays like $r_1^{-\frac{1}{3}}$ instead of $r_1^{-\frac{1}{2}}$.

The Lighthill rule for the radiation condition and the asymptotic formula (8) imply the following. When the wavenumber surface is cylindrical its intersection with the plane $m = 0$ (the wavenumber curve (7)) alone determines the complete pattern except for the amplitudes. At any point $\mathbf{k}_1$ on S, if we draw an *arrow* normal to S and pointing in the direction of σ_0 increasing then this arrow will be along the group velocity of a wave packet centred round $\mathbf{k}_1$. Hence each point $\mathbf{k}_1$ on S corresponds to a plane wave (6) of wavelength $2\pi/|\mathbf{k}_1|$ that could be excited by the forcing effect and would stretch out from the forcing region *in the direction of the arrow at that point*. (Only those points on S at which $\mathscr{H}(l_1, n_1)$ takes a non-negligible value produce significant waves.) Therefore the waves are found in the regions covered by the arrows on S. The arrows at the points of inflexion may form a boundary separating the disturbed and the undisturbed fluid regions. If there is more than one arrow in a particular direction the waves corresponding to these are superposed on one another along that direction and their amplitudes are separately determined by (8).

Further insight regarding the manner in which the different waves propagate may be gained by examining the lines of constant phase

$$\mathbf{k}_1 . \mathbf{r}_1 = \Phi_1 + \sigma_0 t,$$

which are the polar reciprocals of S in a circle of radius Φ, where $\Phi = \Phi_1 + \sigma_0 t$, Φ_1 is a constant and $\mathbf{r}_1 = (x_1, z_1)$. The above equation can be solved and put in the parametric form

$$\mathbf{r}_1 = \Phi^2 \frac{\nabla S}{|\mathbf{k}_1 . \nabla S|} \operatorname{sgn}\left(-\frac{\partial S}{\partial \sigma_0}\right). \tag{9}$$

The sign in the formula given in Lighthill (1967) is corrected so that $\mathbf{r}_1$ is always in the direction of the arrow (the group velocity) and not along the normal.

A qualitative description of the wave pattern excited by the aforesaid forcing effect is given with the help of these rules.

3. Description of wave pattern

The wavenumber curve is always confined to the region $|\sigma_0+n_1| \leqslant 1$, which translates in the negative-n_1 direction as σ_0 increases. The entire frequency spectrum could be divided into three intervals $0 < \sigma_0 < \sin\alpha$, $\sin\alpha < \sigma_0 < 1$ and $\sigma_0 > 1$ such that in any one of these intervals S has the same features for all σ_0 though these features are not the same for different intervals. When $\sigma_0 = \sin\alpha$ there is a degeneracy in the shape of S which has further special features. This is treated separately. First a description of the pattern for a fixed α (say $\alpha = 30°$) and for a typical σ_0 belonging to each of these intervals is given in this section, and the study of the effects due to variations in σ_0 and α are postponed to the next section. The shape of S for $\alpha = 30°$ and for a typical σ_0 belonging to the aforesaid intervals is shown in figures 1, 3, 4 and 5 and the necessary notation used in the text is indicated in the figures. For a non-zero σ_0 the symmetry with respect to the origin present in S when $\sigma_0 = 0$ (cf. Rarity 1967) disappears while $\alpha \neq 0$ or $\frac{1}{2}\pi$ gives asymmetry about the l_1 and n_1 axes.

Let S_+ and S_- represent the two portions of S which are above and below the l_1 axis. By rewriting (7) as

$$\mu = [\pm\sin(\alpha-\theta)-\sigma_0]/\sin\theta, \tag{10}$$

where $l_1 = \mu\cos\theta$ and $n_1 = \mu\sin\theta$, it is not difficult to see that the arrows on the open branches of S point into the regions below it and that for the closed portion they point inwards or outwards according as it lies below or above the l_1 axis. (See figures 1, 3, 4 and 5.) The direction of the arrows jumps from one side to the other as one crosses the origin along either of the branches. Let OR_1–OR_4 denote the directions of the four arrows on S at the origin such that R_1OR_4 is normal to the curve $\mathscr{A}O\mathscr{C}$ and R_2OR_3 to the other. R_1OR_4 and R_2OR_3 make angles $-\phi$ and ϕ respectively with the n axis, where

$$\phi = \cot^{-1}(\sigma_0^{-2}-1)^{\frac{1}{2}}. \tag{11}$$

The direction of the arrow at the point of inflexion will be denoted by OM_i and its inclination to the downstream part of the forcing line by β_i. Let Z_1' denote a point on the downstream part of the forcing line. All the quantities associated with the wavenumber curve are denoted by script capital letters and the corresponding ones in the x_1, z_1 plane by italic capitals.

Case (i). $0 < \sigma_0 < \sin\alpha$

Here S consists of two parabola-like curves, passing through the origin and $\mathscr{C} = (-\sigma_0\cot\alpha, -\sigma_0)$, and asymptotic to $n_1 = -\sigma_0 \pm \sin\alpha$. S_+ has a point of inflexion $\mathscr{M}_1$ to the left of $\mathscr{A}$ and S_- also has a point of inflexion $\mathscr{M}_2$ to the right of $\mathscr{B}$ (see figure 1).

From the shape of S_+ it is easy to see that the associated waves are confined to the bigger of the two wedges R_1OR_2 and R_1OM_1 [viz. R_1OR_2 when $\alpha = 30°$, see figure 2]. There are three waves of different wavelengths along each direction in the smaller of the two wedges $Z_1'OM_1$ and $Z_1'OR_2$ and only one in the other

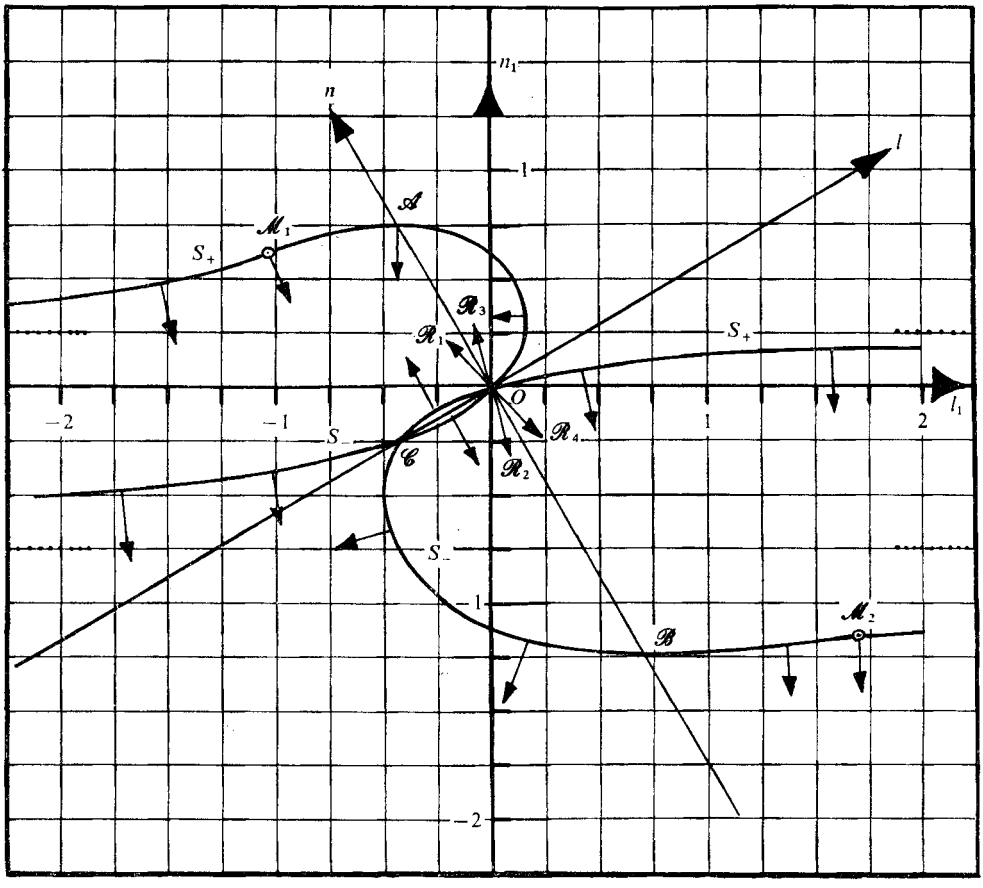

FIGURE 1. The wavenumber curve S for $\sigma_0 = \frac{1}{2}\sin\alpha$ and $\alpha = 30°$. $\cdots$, asymptotes; $\odot$, points of inflexion. The arrows on S give the direction of the group velocity.

directions. The parametric equation (9) for the lines of constant phase in the present problem simplifies to

$$\left.\begin{aligned} x_1 &= \pm\,\Phi^2[1-(\sigma_0+n_1)^2]^{\frac{1}{2}}\,\mathrm{sgn}\,[-(\sigma_0+n_1)]/(l_1^2+n_1^2),\\ z_1 &= -\left(\Phi^2\frac{1}{|n_1|}+\frac{l_1}{n_1}x_1\right), \end{aligned}\right\} \tag{12}$$

with

$$l_1 = \frac{-n_1\sin\alpha\cos\alpha \pm |n_1(\sigma_0+n_1)|\,[1-(\sigma_0+n_1)^2]^{\frac{1}{2}}}{[(\sigma_0+n_1)^2-\sin^2\alpha]} \tag{13}$$

and $|\sigma_0+n_1| \leqslant 1$. A typical wave-crest shape P_1, given by (12), is shown in figure 2. It is a cusp-shaped curve with its arms asymptotic to OR_1 and OR_2 and with OM_1 as the cusp locus. Directed lines drawn normal to P_1 represent, both in magnitude and direction, the phase velocity

$$\mathbf{V}_p = \mu^{-1}(\sigma_0+\mu\sin\theta)\,\hat{\mathbf{k}}_1 \tag{14}$$

of the waves relative to the fluid at that point, where $\hat{\mathbf{k}}_1$ is the unit wavenumber vector. The entire family of these crests touches the downstream part of the

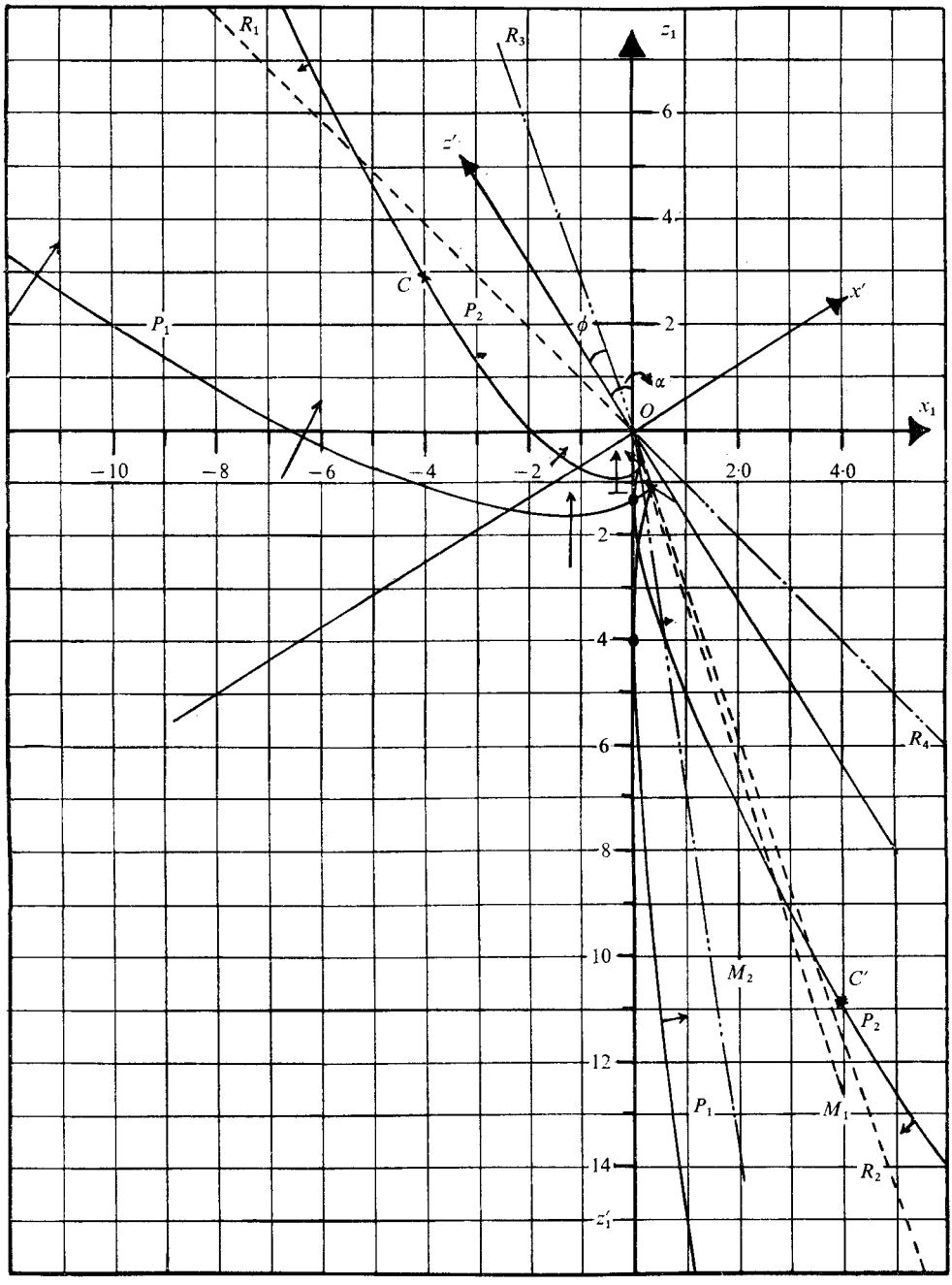

FIGURE 2. The shape of the lines of constant phase corresponding to S in figure 1. ●, caustic points; →, magnitude and direction of phase velocity at that point; |→, maximum phase velocity; ×, points C and C'. The various lines which determine the enveloping wedge of a particular system have the same notation. The x' and z' axes are parallel to the x and z axes but fixed in the forcing effect.

forcing line, forming a caustic along it. The waves of minimum wavelength and zero phase velocity are found near the caustic point, denoted by a solid circle, and the wavelength and phase velocity increase without limit towards OR_1 or OR_2. In particular, the crests which are to the left of the forcing line travel with speeds much greater than U. The part of the wave crests above the caustic point moves towards the forcing line while the portion below moves away from it. This leads to accumulation of wave crests to the right of the downstream part of the forcing line. Thus the waves associated with S_+ consist of a single system of waves, say system I, propagating in a wedge containing the third quadrant. This system includes certain waves with very low wavenumbers propagating ahead of the forcing effect in the second quadrant without penetrating into the wedge Z_1OR_1.

Similarly, the waves associated with S_- propagate in all directions without penetrating into the smaller of the two wedges R_3OR_4 and R_3OM_2, which always includes the first quadrant. (For $\alpha = 30°$ this wedge is given by R_3OR_4 in figure 2.) The crests P_2 are cusped curves with their arms asymptotic to OR_3 and OR_4, OM_2 being the cusp locus. This system, say system II, has a caustic along the downstream part of the forcing line (the caustic point being denoted by a solid circle in figure 2), which leads to accumulation of crests to the right of it. The variation of the wavelength along P_2 is similar to that along P_1 but the nature of the phase velocities is quite different. An interesting feature is that the waves corresponding to $\mathscr{C}$ which are propagating along the directions OC and OC' inclined at angles $\pi + \psi_1$ and $-\psi_2$ to the forcing line are independent of time and have zero phase velocity relative to the fluid, where

$$\psi_{1,2} = \cot^{-1}[(\sin\alpha\cos\alpha \pm \sigma_0)/\sin^2\alpha]. \tag{15}$$

The phase velocity changes its direction to the opposite side as one passes C or C'. The crest within CC' propagates upstream with a speed much less than U while the portion outside CC' travels in the opposite direction with a speed increasing gradually to infinity as one moves towards OR_3 or OR_4. Waves with low wavenumbers, associated with the curve $\mathscr{B}\mathscr{C}O$, have a tendency to influence the upstream side in the second quadrant without penetrating into the wedge Z_1OR_3. The fluid region that could be disturbed by this system is always bigger than that for system I.

Case (ii). $\sin\alpha < \sigma_0 \leqslant 1$

The wavenumber curve consists of two infinite curves. The upper one is a nodal curve with its head above the l_1 axis and with the origin as the nodal point. The 'legs', which are below the l_1 axis, are asymptotic to $n_1 = \pm\sin\alpha - \sigma_0$. The lower curve passing through $\mathscr{C}$, the double point of S, and $\mathscr{B}$ goes to $\pm\infty$ and is asymptotic to $n_1 = \mp\sin\alpha - \sigma_0$. It has two points of inflexion $\mathscr{M}_2$ and $\mathscr{M}_3$ which are on either side of the n axis (see figure 3).

The waves associated with the lower curve propagate in all directions in the wedge M_2OM_3 and there are two waves of different wavelength along each direction. The waves associated with the left and right 'legs' of the nodal curve propagate respectively in the wedges $Z_1'OR_4$ and $Z_1'OR_2$ and there is only a single wave along each direction. Hence the waves associated with S_- propagate mostly

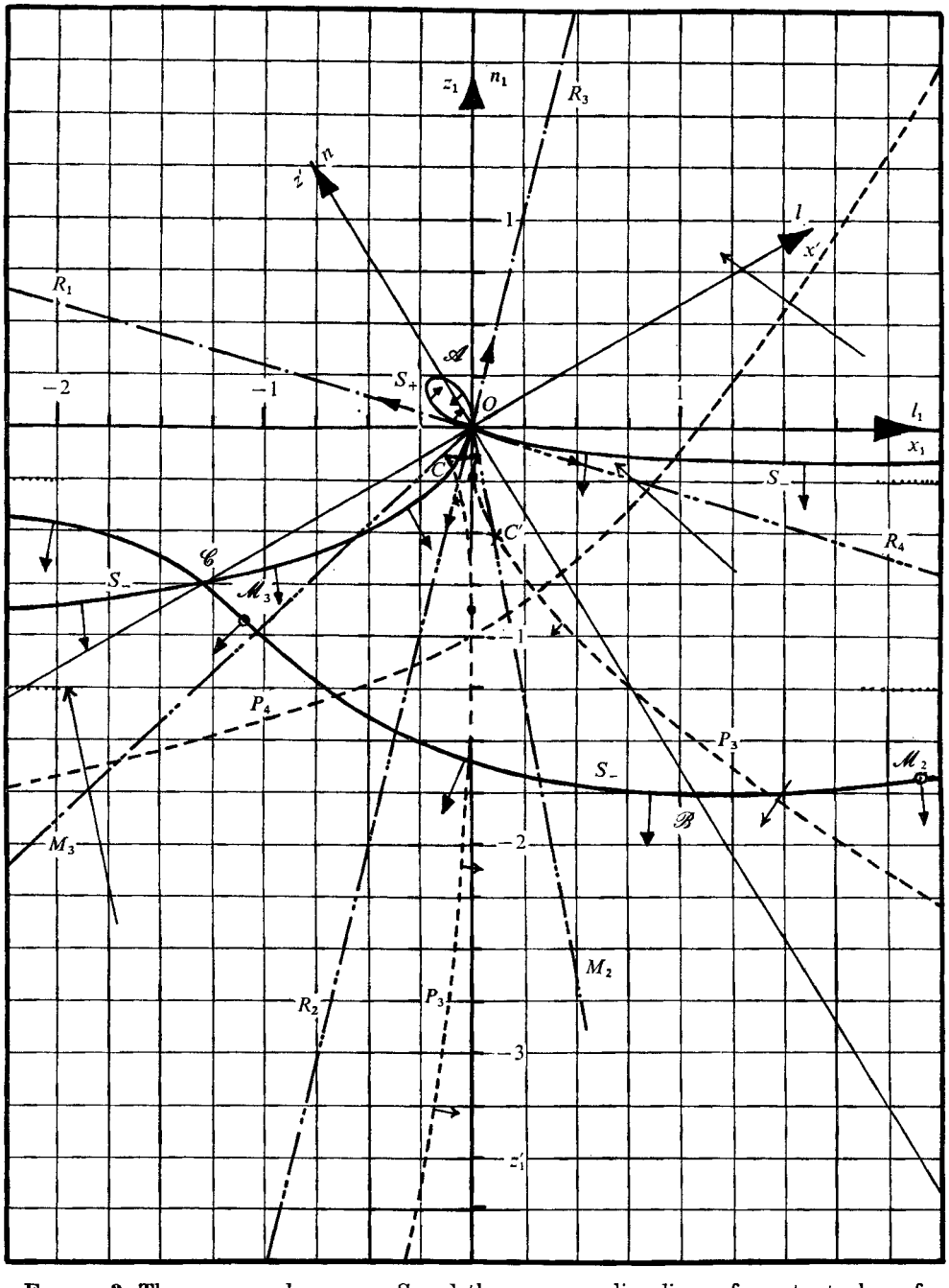

FIGURE 3. The wavenumber curve S and the corresponding lines of constant phase for $\sigma_0 = \frac{1}{2}(1+\sin\alpha)$ and $\alpha = 30°$. ——, S; – – –, lines of constant phase. Other notation as in the figures 1 and 2.

downstream and are confined to the biggest of the wedges formed by OM_3, OR_2, OM_2 and OR_4 (in figure 3 this wedge is given by M_3OR_4). Also in the smallest wedge formed by these directions (R_2OM_2 in figure 3) there are three waves along each direction and there is a concentration of disturbance close to the downstream part of the forcing line which is conspicuous compared with the rest. The wave crests P_3 are shaped like an infinite inverted funnel with two cusps, the respective cusp loci being OM_2 and OM_3, and they extend asymptotically to OR_2 and OR_4. The wave crests touch the downstream part of the forcing line from either side, forming a caustic along it from both sides. The caustic points are denoted by solid circles in figure 3 and the phase velocities are also indicated therein. The portion between the caustic points corresponds to the lower curve and that outside to the 'legs'. As in the previous case the waves along OC and OC', the two directions indicated by the arrows at $\mathscr{C}$, have zero phase velocity and as one moves along P_3, $\mathbf{V}_p$ changes its direction four times. The portions of P_3 below C' and the lower caustic point move towards the downstream part of the forcing line; the portion between C and the upper caustic point moves in the direction of the forcing effect, while the other portions move away from the downstream part of the forcing line. Even though there is an accumulation of crests on both sides of the downstream part of the forcing line this is more marked on the left side. The shorter waves are found close to the forcing line while the longer ones are found close to OR_2 and OR_4. Thus the system III associated with S_- propagates mainly downstream with inverted-funnel-shaped crests.

The waves associated with S_+, the head of the nodal curve, propagate in all directions without penetrating into the wedge R_1OR_3 on the upstream side, with parabola-like wave crests, which are asymptotic to OR_1 and OR_3 and which travel in the same direction as that of the forcing effect with speed much greater than U.

When $\sigma_0 = 1$ the nodal curve becomes a cusped curve with a cusp at the origin, the n axis being the common tangent (see figure 4). The lower curve becomes slightly stretched, but otherwise has the same features. Consequently system IV, associated with S_+, disappears completely and system III, associated with S_-, retains the same characteristics except that now the wedge R_2OR_4 coincides with the x' axis, a line fixed in the forcing effect and parallel to the x axis. So for $\sigma_0 = 1$ there is only one system, namely system III, propagating in all directions below the x' axis, its funnel-shaped crests being asymptotic to this line.

Case (iii). $\sigma_0 > 1$

Here the upper branch crosses the origin and lies completely below the l_1 axis. Like the lower branch it also passes through $\mathscr{C}$ and goes to $\pm\infty$, is asymptotic to $n_1 = \pm\sin\alpha - \sigma_0$ and has two points of inflexion $\mathscr{M}_4$ and $\mathscr{M}_5$ on either side of the n axis. Hence system III propagating in all directions below the x' axis folds back on itself and propagates in the wedge M_4OM_5. The waves associated with the lower branch as usual propagate in the wedge M_2OM_3. There are four waves of different wavelength along each direction in the region common to both the wedges and only two outside. The shape of the wave crests P_5 is shown

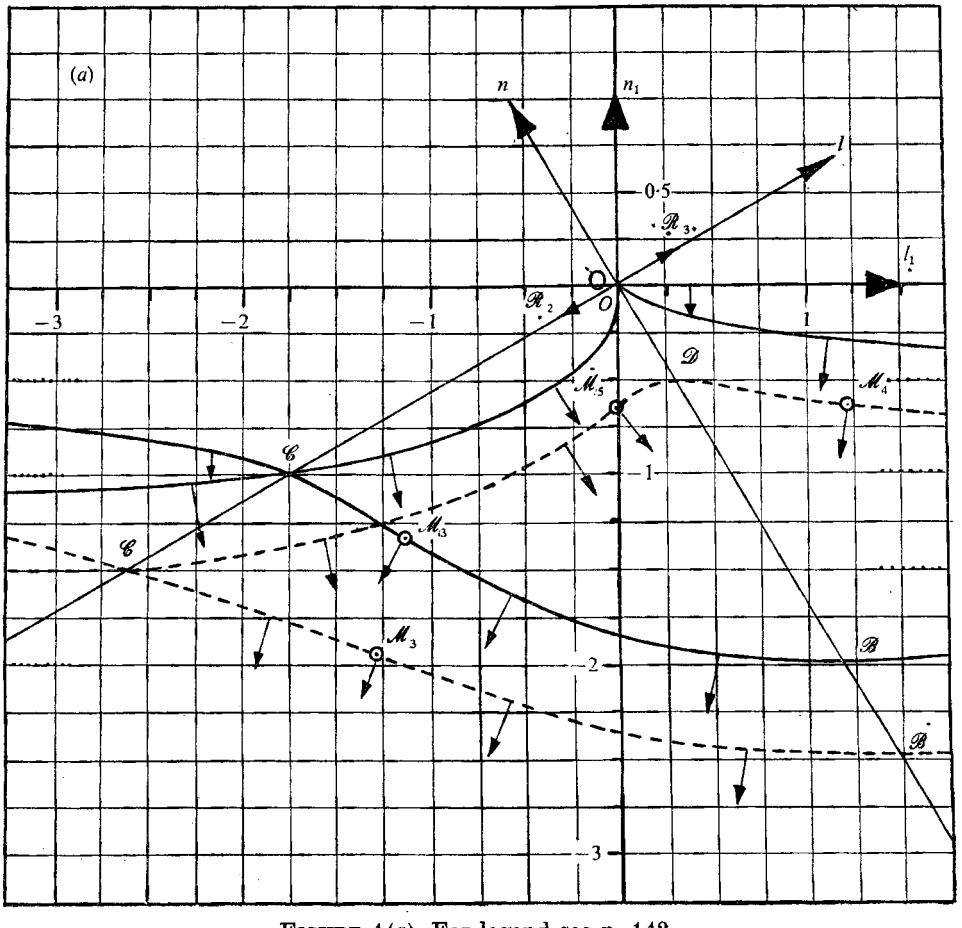

FIGURE 4(*a*). For legend see p. 142.

in figure 4(*b*). It has four cusps, one on each of the boundary lines of M_2OM_3 and M_4OM_5 and touches the downstream part of the forcing line from either side. The portion above the caustic points corresponds to the lower branch of S and the one below to the upper branch. The nature of the phase velocities is similar to that on P_3 with the addition that the new portion M_4M_5 travels downstream. Thus all the waves here reduce to a single system propagating downstream with inverted-funnel-like crests.

Case (iv). $\sigma_0 = \sin\alpha$

In this case the wavenumber curve S splits into two parts: the nodal curve S_n defined by

$$(2\sin\alpha + n_1)\, l_1^2 + l_1 \sin 2\alpha + [(\sin\alpha + n_1)^2 - \cos^2\alpha]\, n_1 = 0 \tag{16}$$

and the straight portion

$$n_1 = 0. \tag{17}$$

S_n has its nodal point at $\mathscr{C}$ and cuts the l_1 axis at two points: the origin and $\mathscr{E}(-\cos\alpha, 0)$. The left and right 'legs' of S_n extend to $\mp\infty$ and are asymptotic to

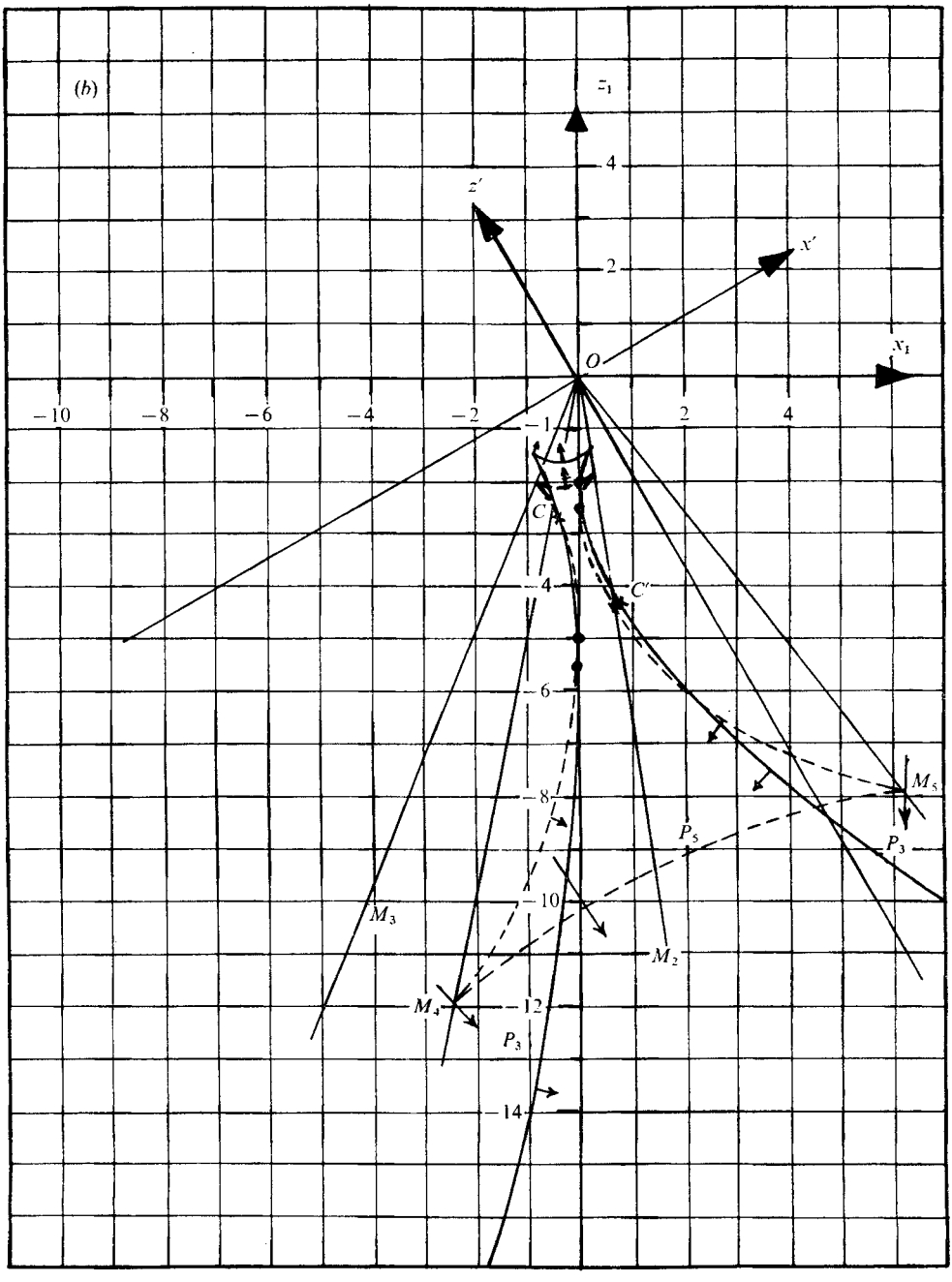

FIGURE 4. Shapes of (*a*) S and (*b*) lines of constant phase for $\alpha = 30°$. ——, $\sigma_0 = 1$; – – –, $\sigma_0 = 1{\cdot}5$.

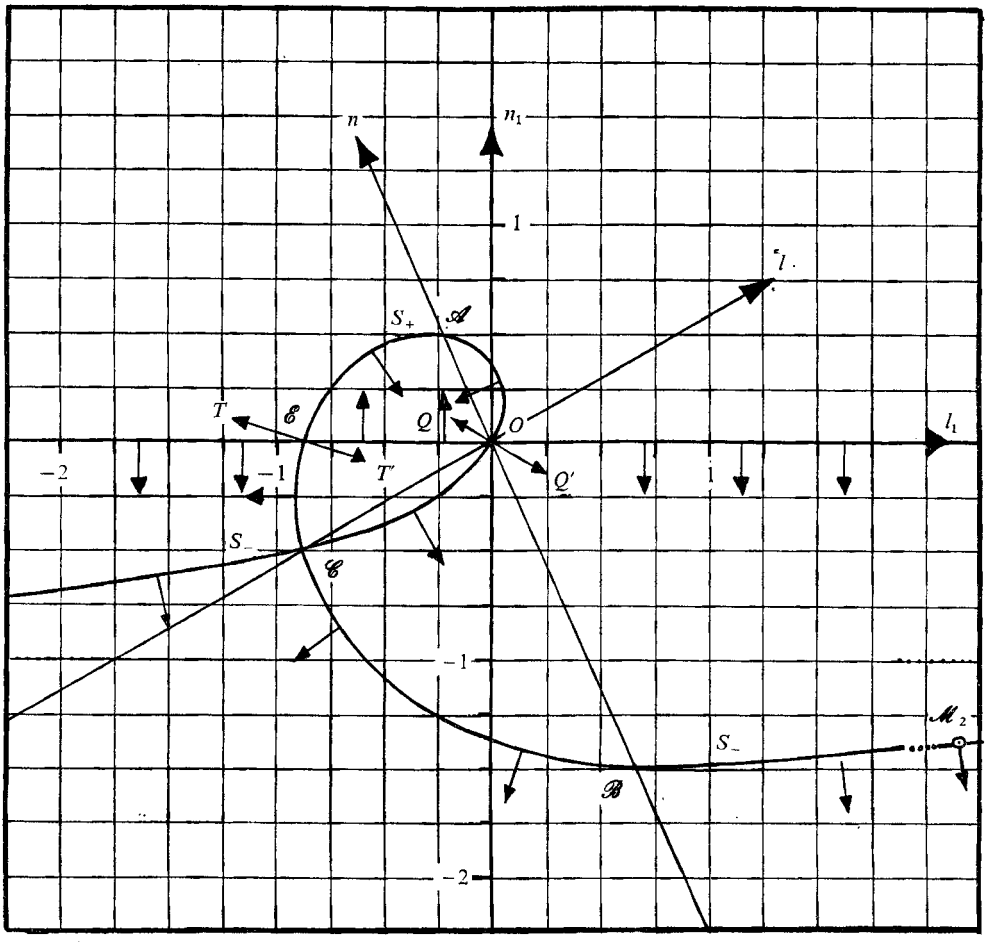

FIGURE 5. The wavenumber curve S for $\sigma_0 = \sin\alpha$ and $\alpha = 30°$. $S_n = S_+ + S_-$.

$n_1 = -\sin\alpha - \sigma_0$. The shape of S and the arrows are shown in figure 5. The arrows on the head of S_n point inwards for the portion above the l_1 axis and outwards for the portion below and downwards for the 'legs'. We shall use the notation S_+ to denote S_n in $n_1 > 0$ and S_- for S_n in $n_1 < 0$. The arrows point upstream on the straight portion (17) within S_n and downstream otherwise. The reason for drawing the arrows in this manner will be clear if we compare the wavenumber curves in figures 3 and 5 and observe that as σ_0 increases the straight line $O\mathscr{E}$ and S_+ become the head of the nodal curve in figure 3; the straight portion to the right of the origin becomes the right 'leg'; the curve $\mathscr{C}\mathscr{E}$ and the straight portion (17) beyond $\mathscr{E}$ become the part of the lower branch, namely, the curve to the left of $\mathscr{C}$. It should be noted that the direction of the arrows jumps from one side to the other as one crosses the origin or $\mathscr{E}$.

Let OT and OT' be the directions pointed by the arrow at $\mathscr{E}$ when $\mathscr{E}$ is approached from $n_1 < 0$ and $n_1 > 0$ respectively. Let QOQ' denote $R_1 O R_4$ when $\sigma_0 = \sin\alpha$. The waves corresponding to S_+ consist of a single system of waves,

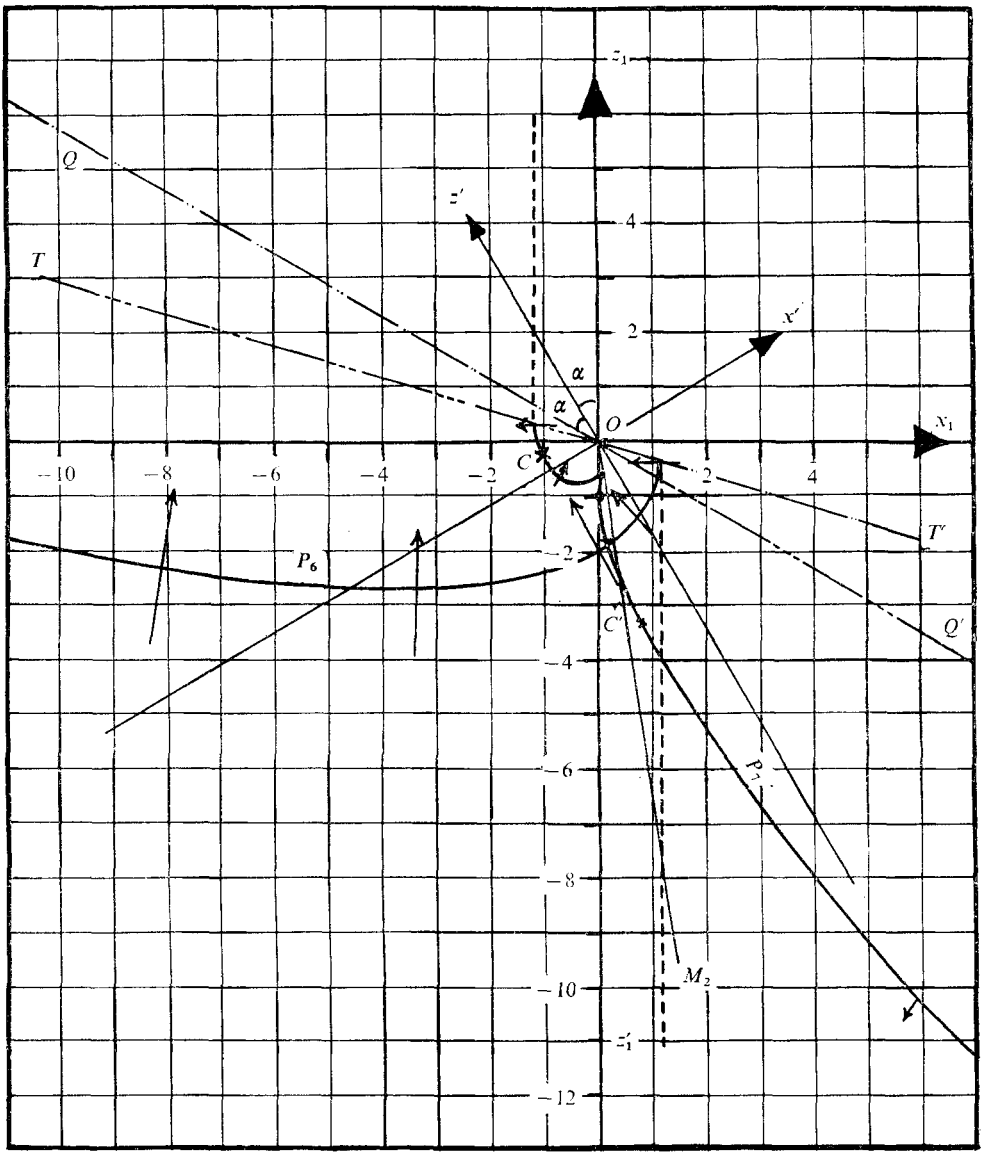

FIGURE 6. A typical shape of the lines of constant phase for $\sigma_0 = \sin\alpha$ and $\alpha = 30°$. The broken lines represent the wave crests in the 'column'.

say system VI, propagating in all directions outside the wedge QOT' with vertex angle $\pi - 2\alpha + \chi$, where $\chi = \cot^{-1}(\frac{1}{2}\tan\alpha)$. This wedge includes the entire first quadrant and part of the second and third quadrants. The shape of the wave crests of this system, say P_6, is shown in figure 6. They all originate at OT' and extend asymptotically to OQ. They travel in the direction of the forcing effect with speeds much greater than U.

The waves corresponding to that branch of S_- which starts from the origin propagate in all directions in $Z_1'OQ'$. The other branch of S_- starting from $\mathscr{E}$

has a point of inflexion $\mathscr{M}_2$ to the right of the n axis. Hence the waves associated with the curve $\mathscr{E}\mathscr{M}_2$ propagate in the wedge TOM_2 and those associated with the curve beyond $\mathscr{M}_2$ propagate in $Z_1'OM_2$. Putting all these facts together we see that the waves associated with S_- consist of a single system of waves, say system VII, mostly propagating downstream in the bigger of the two wedges TOQ' and TOM_2. The associated wave crests P_7 are cusp-shaped with OM_3 as the cuspal locus. Their right arms are asymptotic to OQ' and the left arms terminate on OT (see figure 6). These crests form a caustic along the downstream part of the forcing line. Here again the phase velocity of the waves along the two directions OC and OC' is zero relative to the fluid. The part of P_7 within COC' travels towards the forcing effect and the part outside travels downstream. The phase velocities on P_7 beyond C' increase indefinitely as one moves towards OQ'. The wave crests of both the systems become parallel to the forcing line in TOT'.

The waves associated with the straight portion $n_1 = 0$ are one-dimensional waves of fixed frequency, namely,

$$\exp[i(-t\sin\alpha + l_1 x_1)], \tag{18}$$

which are independent of z_1. The arrows on this portion mean that these waves propagate parallel (either up or down) to the forcing line. All the waves with transverse wavenumbers satisfying

$$-\cos\alpha \leqslant l_1 \leqslant 0 \tag{19}$$

propagate upstream whereas waves with wavenumbers outside (19) propagate downstream. Alternatively, the group velocity

$$\mathscr{U} = -(1 + \cos\alpha/l_1)\,\hat{\mathbf{k}}_1$$

of these waves is either parallel or antiparallel to **U** according as l_1 satisfies (19) or not and hence they propagate in the aforesaid manner.

Each wave originates at some point of the forcing effect and thereafter, being independent of z_1, propagates (either up or down) along a line through that point and parallel to the forcing line. If $x_1 = L_1$ and $x_1 = L_2$, $L_1 < L_2$, are two lines which are separated by a distance L (the transverse dimension of the forcing effect) and enclose the forcing effect then all the waves associated with (17) should be confined to the region between these two lines. The region outside these two lines is not contaminated with the waves with $n_1 = 0$ but it may contain waves associated with S_n. The condition (19) may be rewritten as

$$-\epsilon^{-1}\cos\alpha \leqslant l_1' \leqslant 0,$$

where $l_1 = \epsilon l_1'$ (since all the space and wavenumber variables are stretched by ϵ). This shows that when the transverse dimension L of the forcing effect becomes small (so that ϵ is large) the interval (19) also becomes small and the forcing effect cannot significantly excite upstream waves. But as the transverse dimension increases the waves satisfying (19) can be increasingly excited. The forcing effect excites these waves, and as they are not subjected to any attenuation (because the associated part of the wavenumber curve is a straight line), after a long enough time they extend far upstream and downstream thus forming a 'column' of

waves ahead and behind akin to $\mathscr{T}$ (the two-dimensional counterpart of the Taylor column). The waves in the upstream 'column' are subjected to a low-pass filter which admits only waves satisfying (19), and the downstream ones are subjected to the complementary high-pass filter.

The crests of these waves are always parallel to the forcing line and their phase velocities are given by $\mathbf{V}_p = (\sin\alpha/l_1)\,\hat{\mathbf{i}}$,

where $\hat{\mathbf{i}}$ is a unit vector along the x_1 axis. The phase velocity of the waves with $l_1 > 0$ is in the positive-x_1 direction and each wave crest first appears at $x_1 = L_1$, travels with a speed $\sin\alpha/l_1$ towards $x_1 = L_2$ and disappears at $x_1 = L_2$, whereas for $l_1 < 0$ the situation is the reverse. So the 'column' ahead of the forcing effect is composed of waves whose crests travel from right to left with speeds greater than $\tan\alpha$. But the 'column' behind contains crests which travel in both the directions; those travelling from right to left are slower, with speeds less than $\tan\alpha$, while the speeds of those travelling from left to right range over all values between 0 and ∞.

There is a basic contrast between the structures of the 'column' and $\mathscr{T}$. First, the 'column' is composed of oscillatory (progressive) waves as opposed to steady (standing) waves. The upstream 'column' is subjected to an asymmetric low-pass filter and the downstream $\mathscr{T}$ contains waves of all wavelengths. Besides, on the downstream side there is a superposition of waves over certain wavenumbers, a consequence of the doubly covered nature of the wavenumber curve. This has no counterpart in the present situation. Nevertheless, in the next section it is shown that when $\alpha \to 0$ the present 'column' does tend to $\mathscr{T}$, thereby showing that the 'column' is a counterpart of $\mathscr{T}$ for an arbitrary inclination of the forcing line.

As was observed by Lighthill (1967), the difficulties experienced in estimating the amplitudes in $\mathscr{T}$ are mainly due to the twice-covered part of the wavenumber surface, whereas for $\alpha \neq 0$ no such situation arises, for the associated wavenumber curve is a single straight line $n_1 = 0$. If the integral (3), after $\sigma_0 = \sin\alpha$ has been invoked and $S(\,)$ replaced by $n_1 S_n(\,)$, is evaluated then it may be seen that for the waves associated with $n_1 = 0$ the main contribution comes from the simple pole $n_1 = 0$. This simple pole moves into the upper half of the complex-n_1 plane when σ_0 is changed to $\sigma_0 + i\delta$ if (19) is satisfied, otherwise it moves into the lower half-plane. Thus one gets

$$\mathbf{q}_1 = \begin{cases} \pi e^{-it\sin\alpha}\,\mathbf{I}_1 & \text{for} \quad z_1 > 0, \\ \pi e^{-it\sin\alpha}\,(\mathbf{I}_1 + \mathbf{I}_2) & \text{for} \quad z_1 < 0, \end{cases}$$

where

$$\mathbf{I}_1 = \int_{-\cos\alpha}^{0} i\mathbf{J}\, e^{il_1 x_1}\, dl_1,$$

$$\mathbf{I}_2 = \int_{-\infty}^{-\cos\alpha} (-i)\,\mathbf{J}\, e^{il_1 x_1}\, dl_1,$$

$$\mathbf{I}_3 = \int_{0}^{\infty} (-i)\,\mathbf{J}\, e^{il_1 x_1}\, dl_1$$

and

$$\mathbf{J} = \frac{\mathscr{H}(l_1, 0, \sin\alpha, \alpha)}{l_1 \sin\alpha (l_1 + \cos\alpha)}.$$

Here we notice that the disturbances are progressively amplified on the upstream side as $l_1 \to (-\cos\alpha)_+$ and on the downstream side as $l_1 \to (-\cos\alpha)_-$ even though no waves appear on the upstream or downstream side for values beyond these limits. Lighthill (1967) reasons that this is due to the fact that a forcing effect of given transverse dimensions can excite a wave component most powerfully when the group velocity is very close to the speed of the forcing effect because the time available for the wave component to escape from the forcing effect is then the greatest. However, mechanisms like dissipation, nonlinearity or finite duration of the forcing effect would generally restrict the amplitudes from attaining extremely large values around such wavenumbers.

4. The effect of varying α and σ_0 on the wave pattern

The wave pattern in the two extreme cases $\alpha = 0$ and $\alpha = \frac{1}{2}\pi$, which could be derived from Nigam & Nigam (1962) and Stevenson (1969), is given briefly in the introduction. In this section it is shown how the pattern described in § 3 is altered in the two extreme cases $\alpha = 0$ and $\alpha = \frac{1}{2}\pi$. Incidentally this helps one envisage the nature of the pattern for general α. Also the modifications brought into the pattern as σ_0 varies (α being fixed) are also pointed out.

As σ_0 increases the entire region $|\sigma_0 + n_1| \leqslant 1$ containing S moves in the negative-n_1 direction. Also S is constrained to cross the l_1 axis only through the origin. These two features bring about certain important changes in the shape of S and hence in the pattern. A consequence of this translation is that the wavelength of waves associated with S_+ increases while that corresponding to S_- decreases. Another important point is the nature of the arrows at the origin, which in some cases determines the enveloping wedge. The two directions R_1OR_4 and R_2OR_3 are always equally inclined to the n axis and are independent of α. But as σ_0 increases they turn away from the n axis, coinciding with QOQ' and the forcing line respectively when $\sigma_0 = \sin\alpha$. When $\sigma_0 = 1$, they both coincide with the x' axis. But when α varies, σ_0 being fixed, they simply rotate rigidly about the origin. The variation of ϕ is shown in figure 7.

Case (i). $0 < \sigma_0 < \sin\alpha$

As σ_0 increases towards $\sin\alpha$, S_+ in figure 1 undergoes the following changes. The asymptote $n_1 = \sin\alpha - \sigma_0$ tends to the l_1 axis and the point of inflexion $\mathscr{M}_1$ tends to $\mathscr{E}$ (figure 5). Also the right branch of S_+ tends to the l_1 axis, the curve beyond $\mathscr{M}_1$ on the left branch tends to the negative-l_1 axis beyond $\mathscr{E}$ and the curve $O\mathscr{A}\mathscr{M}_1$ becomes $O\mathscr{A}\mathscr{E}$ in figure 5. In the limit $\sigma_0 \to \sin\alpha$ all the above quantities coalesce with their respective limits. Consequently the cusp locus OM_1 turns away from the downstream part of the forcing line and coincides with OT' when $\sigma_0 = \sin\alpha$. If $\sigma_1(\alpha)$ represents the locus of the point of intersection of β_1 and $\phi - \alpha$ (the points denoted by small circles in figure 7) then it is not difficult to see from figures 7–9 that for $\alpha > 19°$ and $\sigma_0 < \sigma_1(\alpha)$ system I is confined to the wedge R_1OR_2, whose vertex angle $\pi - 2\phi$ decreases as σ_0 increases; whereas for all other α and σ_0 it is confined to R_1OM_1, of vertex angle $\pi - \alpha - \phi + \beta_1$, and

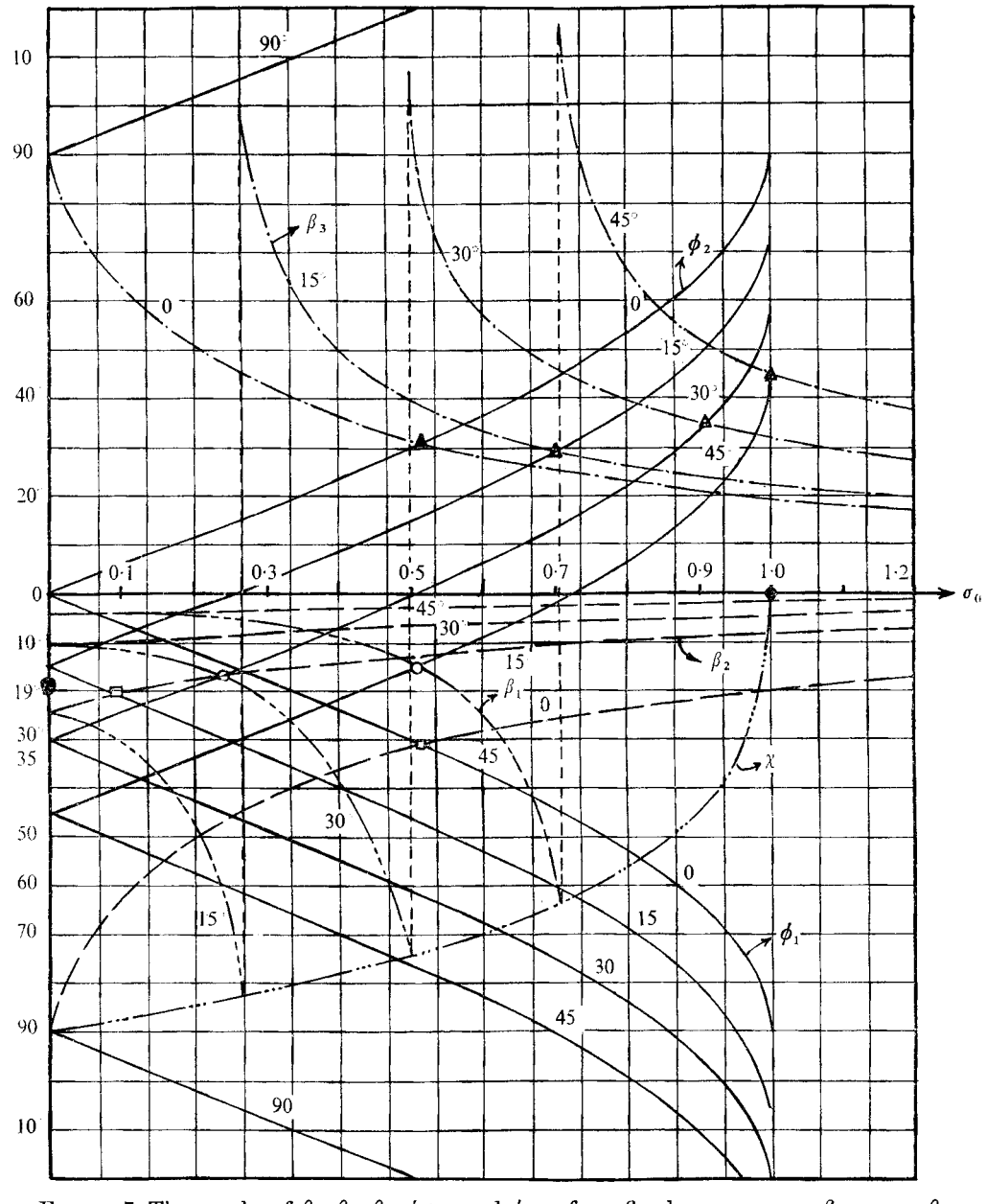

FIGURE 7. The graphs of β_1, β_2, β_3, $\phi+\alpha$ and $\phi-\alpha$ for a fixed α. — · · · —, β_1; — —, β_2; — · —, β_3; ——, $\phi+\alpha$. The numbers on the curves denote the value of α. Points of intersection: ○, β_1 and $\phi-\alpha$; □, β_2 and $\phi+\alpha$; △, β_3 and $\phi-\alpha$.

this widens to coincide with $T'OQ$ as $\sigma_0 \to \sin\alpha$. The two arms of P_1, like OR_1 and OR_2, move towards the downstream part of the forcing line while the cusp moves away. The phase velocities increase as σ_0 increases. A comparison of P_1 and P_6 shows that as $\sigma_0 \to \sin\alpha$ the caustic point tends to $-\infty$ along the downstream part of the forcing line and the portion between the cusp and the caustic

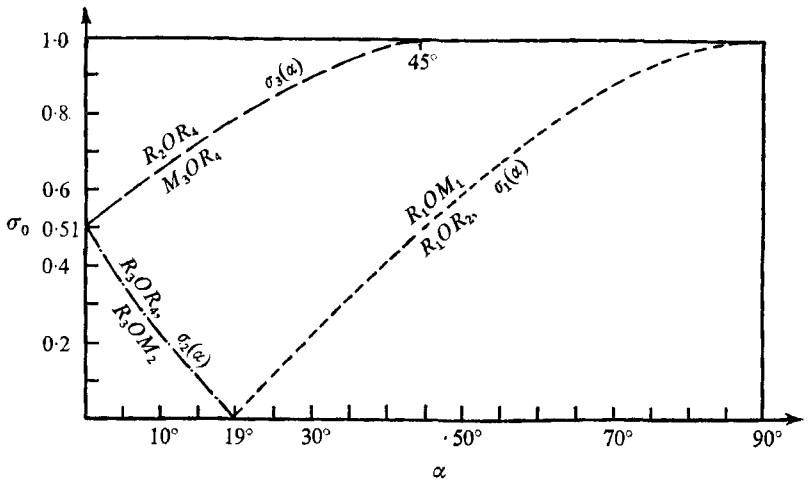

FIGURE 8. The graphs of $\sigma_1(\alpha)$, $\sigma_2(\alpha)$ and $\sigma_3(\alpha)$. The letters written on either side of a curve give the enveloping wedge of the associated wave system for the values of α and σ_0 on that side.

point tends to become parallel to the forcing line while the cusp moves onto OT'. Thus when $\sigma_0 = \sin\alpha$ this system splits into two parts. The waves associated with the curve $O\mathscr{A}\mathscr{M}_1$ become system VI and the rest become straight waves propagating in the downstream 'column' (cf. case (iv) of § 3).

As σ_0 increases the asymptote $n_1 = -\sin\alpha - \sigma_0$ of S_- moves downwards. So does the whole of S_- except the curve $O\mathscr{C}$, which is to the left of the l axis. This curve $O\mathscr{C}$ moves towards the l_1 axis and when $\sigma_0 = \sin\alpha$ becomes the curve $O\mathscr{E}\mathscr{C}$, which has a corner at $\mathscr{E}$ (see figure 5). The graphs of β_2, the angle between OM_2 and the downstream part of the forcing line, are shown in figure 7. This β_2 has a maximum value of $\frac{1}{2}\pi$ when $\alpha = 0$ and $\sigma_0 = 0$ and decreases as α and/or σ_0 increases. If $\sigma_2(\alpha)$ denotes the locus of the point of intersection of β_2 and $\alpha+\phi$ (the points denoted by squares in figure 7) then from figures 7, 8 and 2 it may be seen that for $\alpha < 19°$ and $\sigma_0 < \sigma_2(\alpha)$ system II propagates outside the wedge R_3OM_2, of vertex angle $\pi+\alpha-\phi-\beta_2$, which increases as $\sigma_0 \to \sigma_2(\alpha)$. For all other α and σ_0 it propagates outside R_3OR_4, which shrinks towards Z_1OQ' (in figure 6) as $\sigma_0 \to \sin\alpha$ and whose vertex angle $\pi - 2\phi$ decreases to $\pi - 2\alpha$. Thus for all α, the region influenced by system II diminishes or spreads out as σ_0 increases according as it propagates outside R_3OM_2 or outside R_3OR_4. The arms of P_2 turn outwards, occupying larger regions; in particular the arm asymptotic to OR_3 tends to become parallel to the forcing line and the cusp locus turns towards the downstream part of the forcing line. The wave crests slow down as σ_0 increases. When $\sigma_0 = \sin\alpha$ this system splits into two parts. Part of the waves associated with the curve to the left of $O\mathscr{C}$ become straight waves in the upstream 'column' while the rest become system VII (cf. case (iv), § 3).

When σ_0 decreases the wavenumber curve and the pattern undergo changes which are exactly opposite to those described above. The double point $\mathscr{C}$ moves towards the origin and coincides with it when $\sigma_0 = 0$, and S becomes symmetric

about the origin. That is, whenever $\mathbf{k}_1$ is a point on S, $-\mathbf{k}_1$ is also on S and the arrows at the two points are in the same direction. Hence the wave systems associated with S_+ and S_- become identical (cf. § 1). So as $\sigma_0 \to 0$ systems I and II tend towards each other and collapse into a single system which is actually a superposition of two identical wave systems.† Hence for all α the periodic nature of the forcing effect splits the waves into two systems which are otherwise coincident.

The two wave systems I and II are possible only when $\alpha \neq 0$. Here it will be shown how these systems change with α. For a fixed σ_0 the region $|\sigma_0 + n_1| \leqslant 1$ containing S does not change with α but as α increases the l and n axes and S in the neighbourhood of the origin rotate about the origin in the anticlockwise sense, effecting the following changes. The two points

$$\mathscr{A} = [-(1-\sigma_0)\tan\alpha, -(1-\sigma_0)] \quad \text{and} \quad \mathscr{B} = [(1+\sigma_0)\tan\alpha, -(1+\sigma_0)]$$

move away from the n_1 axis along the lines $n_1 = \pm(1-\sigma_0)$ respectively and $\mathscr{C} = [-\sigma_0 \cot\alpha, -\sigma_0]$ moves towards the n_1 axis along $n_1 = -\sigma_0$. The two asymptotes move away from each other. Consequently the two branches without points of inflexion move away from the l_1 axis and bend more in the neighbourhood of the origin. The curve $\mathscr{A}O\mathscr{B}$ moves inwards while the curves beyond $\mathscr{A}$ and $\mathscr{B}$ get squeezed between the lines $n_1 = \pm(1-\sigma_0)$ and their respective asymptotes. In this process $\mathscr{M}_1$ and $\mathscr{M}_2$ move away from the n_1 axis, the arrows at these points tend to become parallel to the n_1 axis and the whole of S gets deformed to become symmetric about the l axis. Finally when $\alpha \to \frac{1}{2}\pi$ the l and n axes coincide with the n_1 and l_1 axes; $\mathscr{A}$, $\mathscr{M}_1$ and $\mathscr{B}$, $\mathscr{M}_2$ respectively go to $\mp\infty$; $\mathscr{C}$ moves onto the n_1 axis and the whole of S becomes symmetric about the n_1

† In Subba Rao & Prabhakara Rao (1971) it is pointed out that the group velocities of the waves corresponding to $\mathbf{k}$ and $-\mathbf{k}$ are identical and that the phase velocities are equal in magnitude but opposite in direction. This led to the ambiguity of two phase velocities at each point of the surface of constant phase. This ambiguity was avoided by applying the radiation condition, which was shown to pick only one out of the pair $\pm\mathbf{k}$ to be in agreement with Lighthill's comment. These two conclusions are wrong and they are a consequence of ignoring the sign of $\sigma_0 + Un$. It is not difficult to see that in all the situations concerning this paper whenever there is symmetry with respect to the origin, the phase and the group velocities of the waves with wavenumbers $\pm\mathbf{k}$ are identical and they both satisfy the radiation condition. But this is not in contradiction to the general statement of Lighthill (1960, p. 407, second paragraph) that the situation satisfying the radiation condition takes only one out of the pair $\pm\mathbf{k}$. For, the above statement is true if the wavenumber surface, for a particular frequency, is a closed surface not enclosing any singularities; then the arrows will either be always outwards from the surface or always inwards. This is because the frequency will either increase outwards from the surface or increase inwards. It is in such cases, owing to the symmetry with respect to the origin, where the arrows at $\mathbf{k}$ and $-\mathbf{k}$ will lie in opposite directions, that the above general statement applies and hence only one of them contributes (M. J. Lighthill, private communication). But all the steady-state problems mentioned in this paper (including that of Subba Rao & Prabhakara Rao) are exceptions to the above comment for the wavenumber curve always has a singularity at the origin whether the surface is closed or not. This makes it possible for the frequency to increase inwards on a part of the wavenumber surface and outwards on the other part no matter whether the surface is closed or open. As a result the arrows at $\pm\mathbf{k}$ lie in the same direction and hence the two waves are superposed and in that direction.

axis as was described in the introduction (cf. p. 132; $0 < \sigma_0' < 2\Omega$). If α decreases so that $\sin\alpha > \sigma_0$ then S undergoes exactly contrary changes. From (11) it follows that when α increases R_1OR_4 and R_2OR_3 undergo a rigid rotation about the origin along with l and n axes while the cusp loci OM_1 and OM_2 turn towards the downstream part of the forcing line. Therefore the two wedges R_1OR_2 and R_3OR_4 associated respectively with systems I and II simply rotate about the origin through an angle equal to the increase in α. $\sigma_1(\alpha)$ exists only for $\alpha > 19°$ and is an increasing function of α. But $\sigma_2(\alpha)$, defined for $\alpha < 19°$, is a decreasing function of α. This implies that the range of σ_0 for which system I is confined to R_1OR_2 increases with α and the range of σ_0 for which system II is confined to R_3OM_2 decreases.

To start with let system I be confined to R_1OM_1. As α increases R_1OM_1 will decrease until $\sigma_1(\alpha) = \sigma_0$, that is, until OM_1 crosses OR_2, and from then on the disturbed region will be confined to R_1OR_2, which will simply rotate about the origin. Like R_1OR_2 the wave crests also rotate in the anticlockwise sense such that they always touch the downstream part of the forcing line. In this process the cusps move towards the downstream part of the forcing line and the caustic points move closer to their respective cusps. When $\alpha = \frac{1}{2}\pi$ the caustic points coincide with the cusps and P_1 becomes symmetric about the downstream part of the forcing line. System II, which propagates outside R_3OR_4 or R_3OM_2 according as $\sigma_2(\alpha) \lesseqgtr \sigma_0$, and the associated crests undergo similar changes. The wavelengths of the waves corresponding to the two portions beyond $\mathscr{A}$ and $\mathscr{B}$ decrease and the wavelengths of the waves associated with the rest of S increase. As α increases the region that could be influenced in the second quadrant by the two systems, particularly system II, diminishes while they gain influence on an almost equally large region in the fourth quadrant. That is to say, as α increases the upstream influence in the second quadrant decreases. This upstream influence for all α and σ_0 depends on the smallness of $\sin\alpha - \sigma_0$; the smaller this quantity the greater is the disturbed region in the second quadrant. It must be noted that under no circumstances, for $0 < \alpha < \frac{1}{2}\pi$, will systems I and II be able to penetrate into the first quadrant.

Case (ii). $\sin\alpha < \sigma_0 < 1$

The head S_+ of the nodal curve shrinks to the origin when $\sigma_0 \to 1$ and the arrows at the origin turn away from the n axis to coincide with the l axis. So the wedge R_1OR_3, which is free of system IV, is compressed towards the region below the x' axis (a line perpendicular to the axis of rotation) and the influence of this system on the upstream side, particularly on the first quadrant, decreases. The wave crests are straightened and move further down from the forcing effect. This system disappears completely when $\sigma_0 = 1$. The wavelengths and the phase velocities of this system increase indefinitely as $\sigma_0 \to 1$. When $\sigma_0 \to \sin\alpha$, S_+ expands and becomes the straight portion $O\mathscr{E}$ and the curve $\mathscr{E}\mathscr{A}O$ above it. Now the wedge R_1OR_3, the wave crests P_3 and all other related quantities undergo changes exactly opposite to those in the case $\sigma_0 \to 1$. When σ_0 is sufficiently close to $\sin\alpha$ this system influences the entire plane except for

the small wedge R_1OR_3 in the second quadrant. When $\sigma_0 \to \sin\alpha$, in the neighbourhood of $\mathscr{E}$, S_+ develops a sharp bend which becomes the corner at $\mathscr{E}$. For this reason all the waves propagating along various directions in the first quadrant, except those parallel to the forcing line, are eliminated. Thus when $\sigma_0 \to \sin\alpha$ the pattern splits into the straight waves in the upstream 'column' and system VI. The portion of P_3 in the first quadrant becomes parallel to the forcing line while the rest becomes P_6.

The modifications to S_- brought about when $\sigma_0 \to 1$ may be seen easily by comparing S_- in figures 3 and 4. The angles β_2 and β_3 are largest when $\sigma_0 = \sin\alpha$ and decrease gradually as $\sigma_0 \to 1$ (cf. figure 7). Therefore the cusp loci OM_2 and OM_3 turn towards the downstream part of the forcing line while the wedge R_2OR_4 widens to coincide with the x' axis. The portion of P_3 lying between the cusps shrinks and the parts going to infinity turn outwards until they become asymptotic to the x' axis. The wavelengths and phase velocities of waves propagating along any direction decrease. If $\sigma_3(\alpha)$ denotes the locus of the point of intersection of β_3 and $\phi - \alpha$ (the points denoted by triangles in figure 7) then from figures 3, 7 and 8 the following may be seen. For $\alpha > 45°$ the system is confined to R_2OR_4 for all σ_0. If $19° < \alpha < 45°$ then the system is confined to M_3OR_4 for $\sigma_0 < \sigma_3$ and to R_2OR_4 for $\sigma_0 > \sigma_3$. But if $\alpha < 19°$ then it is confined to M_3OM_2, M_3OR_4 or R_2OR_4 according as $\sin\alpha < \sigma_0 < \sigma_2, \sigma_2 < \sigma_0 < \sigma_3$ or $\sigma_3 < \sigma_0 < 1$. As σ_0 increases the wedges M_3OM_2 and M_3OR_4 shrink whereas R_2OR_4 widens. When $\sigma_0 \to \sin\alpha$ the right 'leg' of S_- in figure 3 tends to the positive-l_1 axis and the curve beyond $\mathscr{C}$ of the lower branch goes into the curve $\mathscr{C}\mathscr{E}$ and the straight portion beyond $\mathscr{E}$ (cf. figure 5). The rest of S_- simply moves upwards with minor changes. So when σ_0 increases slightly from $\sin\alpha$ the straight waves in the downstream 'column' and system VII combine to form system III. This is because the corner at $\mathscr{E}$ becomes a smooth bend and the waves associated with this bend will propagate in the third quadrant, filling the gap between the downstream 'column' and system VII to form system III. The straight waves in the downstream 'column' with $l_1 < -\cos\alpha$ and $l_1 > 0$ will now become waves propagating to the left of the downstream part of the forcing line, the corresponding parts of P_3 being the curve between C and the caustic point, and the portion below the caustic point respectively.

Keeping σ_0 fixed if α is allowed to decrease to zero the nodal curve rotates about the origin in the clockwise sense while the lower branch rotates in the anticlockwise sense so that $\mathscr{B}$ moves to the n_1 axis, $\mathscr{C}$ goes to $-\infty$ and both the asymptotes move towards each other, making S symmetric about the n_1 axis. In this process the wedge R_2OR_4 rotates rigidly about the origin while OM_3 turns towards the downstream part of the forcing line and OM_2 turns away so that β_3 and β_2 tend to become equal. The wave crests P_3 also rotate in the clockwise sense in such a way that they always touch the downstream part of the forcing line from either side. The caustic points move towards each other and coincide when $\alpha = 0$, and the entire wave pattern becomes symmetric about the downstream part of the forcing line as was pointed out in the introduction for $0 < \sigma_0' < 2\Omega$. The wavelengths and phase velocities of waves associated with the right 'leg' and the lower branch in $l_1 < 0$ increase and for the rest of S_- they

decrease. S_- and the associated wave pattern undergo exactly reverse changes when α increases such that $\sin\alpha < \sigma_0$. System IV also simply rotates clockwise about the origin and tends to become symmetric about the downstream part of the forcing line. As a result the upstream influence in the third quadrant decreases. The phase velocities and the wavelengths associated with this system increase. The crests P_4 move slightly away from the forcing effect. Here again the upstream influence due to system IV in the first quadrant depends on the smallness of the quantity $\sigma_0 - \sin\alpha$.

Case (iii). $\sigma_0 > 1$

As σ_0 increases, owing to the downward motion of S, the points $\mathscr{A}$, $\mathscr{B}$ and $\mathscr{C}$ move farther and farther from the n_1 axis, stretching the two branches of S. All the cusp loci turn towards the downstream part of the forcing line, diminishing the extent of the disturbed region. The wave crests also accordingly shrink in size and move closer to the forcing effect. The wavelengths and phase velocities of the waves in any particular direction decrease as σ_0 increases. When α increases (decreases) the entire wave crest rotates in the clockwise (anticlockwise) sense such that it always touches the downstream part of the forcing line from either side. When $\alpha = 0$ or $\alpha = \frac{1}{2}\pi$, we recover the patterns described for $\sigma_0' > 2\Omega$ in the introduction.

Case (iv). $\sigma_0 = \sin\alpha$

The wavenumber curve associated with the pattern generated by a steady forcing effect travelling along the axis of rotation consists of a unit circle (the radius of the circle would be $2\Omega/U$ in terms of dimensional variables) and two coincident lines or a sphere and two coincident planes when the forcing effect is axisymmetric (cf. Rarity 1967; Lighthill 1967). The waves associated with the circle consist of two identical wave systems, superposed on each other, of cylindrical waves of wavelength $\pi U/\Omega$ propagating in all directions below the forcing effect with semicircular wave crests. The waves associated with the straight portion propagate within $\mathscr{T}$. If a distinction is made between the two coincident lines then according to the Lighthill (1967) one of the lines has all its arrows pointing downwards while on the other line they point upwards on the portion within the circle and downwards on the rest. This implies that there are two waves of the same wavelength corresponding to each point on the coincident lines, and if they are associated with a point on these lines outside the circle then they are found on the downstream side superposed on one another but if they correspond to the points within the circle then one of them is found on the upstream $\mathscr{T}$ and the other downstream.

When $\alpha \to 0$ it is natural to expect the 'column' and systems VI and VII to become $\mathscr{T}$ and the cylindrical waves. One may at once observe that when $\alpha = 0$ equation (7) reduces to a circle and two coincident lines. But greater insight may be gained regarding how the additional waves in $\mathscr{T}$, absent in the 'column', would split up from the other systems and be added to form $\mathscr{T}$. This is done by observing how the wavenumber curve in figure 5 becomes a circle and two coincident lines

when $\alpha \to 0$ (unless otherwise stated the centres of all the circles mentioned will always be at the origin). A further study of S with $\alpha \to \frac{1}{2}\pi$ would help one to envisage the wave pattern for any α.

When $\alpha \to 0$, S_n is subjected to a rotation as well as a translation, since $\sigma_0 = \sin\alpha \to 0$. The asymptote $n_1 = -2\sin\alpha$ moves towards $n_1 = 0$. The entire head of S_n enlarges and rotates clockwise about the origin. In this process $\mathscr{A} \to (0, 1)$, $\mathscr{B} \to (0, -1)$, $\mathscr{C} \to \mathscr{E} \to (-1, 0)$ and $\mathscr{M}_2 \to (1, 0)$. Consequently the curve $O\mathscr{C}$ and the left leg of S_n become the negative-l_1 axis. The rest of the head, $O\mathscr{A}\mathscr{E}\mathscr{C}$, owing to the rotation and the enlargement, becomes the part of the l_1 axis between the origin and $(1, 0)$ and the unit semicircle in $n_1 > 0$. The curve $\mathscr{C}\mathscr{B}\mathscr{M}_2$ becomes the unit semicircle in $n_1 < 0$ and the curve beyond $\mathscr{M}_2$ becomes the l_1 axis beyond $(1, 0)$. The arrows at the origin turn (clockwise) towards the n_1 axis and the arrows at $\mathscr{E}$ turn (anticlockwise) towards the l_1 axis. The wavenumber spectrum $(-\cos\alpha, 0)$ enlarges to $(-1, 0)$. Also, since the portion of the head in the first quadrant goes into $n_1 = 0$, $0 \leqslant l_1 \leqslant 1$ with arrows pointing up and a circular arc when $\alpha = 0$ the spectrum jumps to $(-1, 1)$ as required by Lighthill (1967). Since the arrows lie on the same side of the curve as $\alpha \to 0$ it is not difficult to see that the nature of the arrows also agrees with Lighthill (1967).

The implications of these changes in S with special reference to system VI associated with S_+ are studied here. The wedge $T'OQ$, which is free of this sytem, shrinks towards the first quadrant, thereby spreading the influence of the system over all the other three quadrants. Along with OQ, P_6 curves inwards, its point of intersection with the x_1 axis moves towards the origin, the curve below it tends to a semicircular shape and the part above it tends to become parallel to the forcing line. The wavelength of the waves propagating below decreases towards the uniform value $\pi U/\Omega$. The phase velocities also decrease with α. In the second quadrant a sort of stretching of waves over certain sets of wavenumbers and accumulation around certain others take place. This is because, as $\alpha \to 0$, S_+ develops a sharp smooth bend for sufficiently small α which becomes the corner at $(1, 0)$. The slope almost changes from α to $\frac{1}{2}\pi$ in the neighbourhood of this bend. The portion between the origin and the bend elongates and straightens while the curve above tends to a circular shape. Therefore the density of waves propagating between the negative-x_1 axis and OQ decreases while more and more waves are added to the region below the x_1 axis and the one close to OQ. Moreover, the amplitude of the waves near OQ is less and less attenuated, since the associated wavenumber curve straightens up. Thus, like a rubber sheet which is being stretched the region between the negative-x_1 axis and OQ becomes less and less contaminated with the waves of this system while the region close to OQ is intensified. Finally when $\alpha = 0$ all the intermediate waves vanish, splitting system VI into two, the straight waves with transverse wavenumbers $0 \leqslant l_1 \leqslant 1$ and the cylindrical waves below. Also, the wave spectrum $-\cos\alpha \leqslant l_1 \leqslant 0$ of the waves in the upstream 'column' enlarges to $(-1, 0)$ and the straight waves splitting out from system VI fill the missing gap between the upstream 'column' and the upstream $\mathscr{T}$ while the rest of system VI forms one of the coincident systems of cylindrical waves.

System VII will be divided into two parts: the first associated with the curve

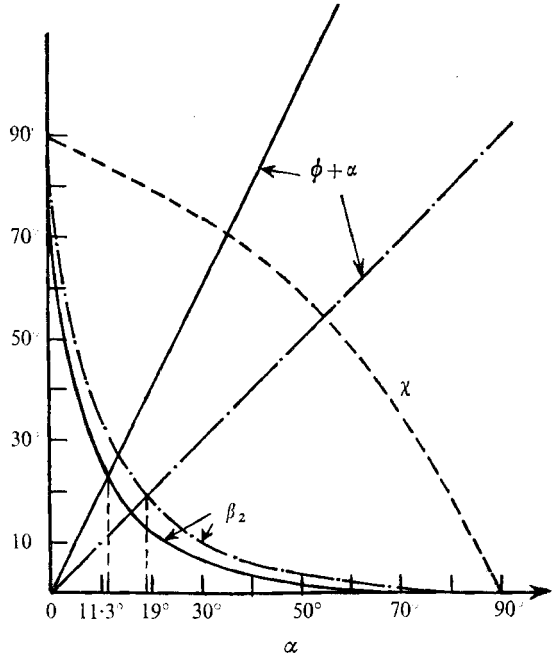

FIGURE 9. Graphs of β_2 and $\phi+\alpha$ for $\sigma_0 = 0$ (solid line) and for $\sigma_0 = \sin\alpha$ (dot-dashed line). The broken line represents the graph of χ, the vertex angle of the wedge Z_1OT.

$\mathscr{E}\mathscr{C}\mathscr{B}\mathscr{M}_2$ and the second with the rest of S_-. Waves in the first part propagate along all directions between OT and OM_2 and the shape of their crests is given by the part of P_7 which is to the left of the cusp. Waves in the second set have the right arm of P_7 as their crests and propagate in the two wedges $Z_1'OM_2$ and $Z_1'OQ'$. From the loci of the points of intersection of the line $\sigma_0 = \sin\alpha$ with β_2 and $\phi+\alpha$ curves (see figures 7 and 9) it may be seen that $\beta_2 > \phi+\alpha$ for $\alpha < 11{\cdot}3°$ and so system VII is confined to TOM_2 and to TOQ' for $\alpha > 11{\cdot}3°$. As α decreases TOM_2 spreads out while TOQ' shrinks. Also, as α decreases the wavelengths of the waves propagating in and close to the wedge TOC increase and the wavelengths of all other waves decrease. The phase velocities in general increase. As $\alpha \to 0$ the waves in the first set spread out to propagate in all directions below the forcing effect (since the associated wavenumber curve becomes the unit semicircle in the lower half-plane), their wavelengths tend to the uniform value $\pi U/\Omega$ and the correspoding wave crests tend to a semicircular shape. Thus this set of the waves becomes the other coincident system of circular waves on the downstream side. The waves belonging to the second part turn towards the downstream part of the forcing line (since the associated wavenumber curve becomes the entire l_1 axis except $0 < l_1 < 1$) and become straight unattenuated waves propagating downstream and are added to the downstream 'column'. The intermediate waves, associated with the bend containing $\mathscr{M}_2$ and propagating between these straight waves and OM_2, become scarce and vanish when $\alpha = 0$ as described above. These straight waves will now fill the gap between the downstream 'column' and the downstream $\mathscr{T}$, eliminating the complementary high-pass filter restriction required by $\mathscr{T}$.

As α increases the whole of S_n, along with the l and n axes, rotates anticlockwise and translates downwards such that $\mathscr{C} \to (0, -1)$ and $\mathscr{B}$ and $\mathscr{M}_2$ move away from the n_1 axis. The head of S_n gradually crosses the l_1 axis making $\mathscr{E}$ and $\mathscr{A}$ tend to the origin. The asymptote also moves downwards and each 'leg' tends to become the image of the other in the l axis. Finally when $\alpha = \frac{1}{2}\pi$ the nodal curve S_n lies completely below the l_1 axis, touching it at the origin, and becomes symmetric about the l axis (and thus the n_1 axis). The points $\mathscr{M}_2$ and $\mathscr{B}$ go to infinity in the positive-l_1 direction and the asymptote becomes $n_1 = -2$. In this process the part of $O\mathscr{E}$ with arrows pointing upwards shrinks gradually to the origin while the portion with arrows downstream increases to cover the entire l_1 axis.

Therefore, as α increases the wavenumber spectrum of the waves in the upstream 'column' decreases, eliminating the shorter waves and adding them to the downstream 'column'. Finally when $\alpha = \frac{1}{2}\pi$ all the waves appearing in the upstream 'column' disappear and so does the upstream 'column' itself while the downstream one persists without any restriction on wavelengths. The two lines QOQ' and TOT', as α increases, rotate in opposite directions to coincide with the forcing line. So the region influenced by system VI gradually decreases. The wavelengths of this system increase without limit, P_6 moves farther and farther from the forcing effect and this system disappears when $\alpha = \frac{1}{2}\pi$. System VII spreads out, influencing larger areas in the first and the second quadrants as OT' and OQ' turn towards the positive-z_1 axis. So this system penetrates into the first quadrant as α exceeds 45° and this influence in the first quadrant increases to affect the entire first quadrant as $\alpha \to \frac{1}{2}\pi$. The cusp locus of P_7 turns towards the downstream part of the forcing line and the arm in the fourth quadrant curves to become asymptotic to Oz_1. Finally when $\alpha = \frac{1}{2}\pi$ this system propagates in all directions with ω-shaped crests which are symmetric about the forcing line, which is a common tangent at the cusps. This wave pattern will be the same as that discussed in the introduction for $\sigma_0' = 2\Omega$.

5. Concluding remarks

For $0 < \sigma_0 < \sin\alpha$ the oscillatory nature of the forcing effect splits the steady-case ($\sigma_0 = 0$) identical wave systems into two. One of these systems propagates in all directions without penetrating into an upstream wedge containing the first quadrant and the other propagates in a wedge below the z' axis, a line parallel to the axis of rotation. The wave crests of both the systems have the shape of a cusped curve. The crests of the first system travel upstream with speeds greater than U whereas those of the other system travel partly upstream and partly downstream. As σ_0 increases towards $\sin\alpha$ the bigger system spreads out to propagate in all directions outside the first quadrant and the other system shrinks. When $\sigma_0 = \sin\alpha$ part of these two systems splits further, forming a family of straight unattenuated waves travelling (up and down) in a 'column' parallel to the forcing line and two other systems.

For $\sin\alpha < \sigma_0 < 1$ there are again two systems of waves, one with inverted-funnel-like crests propagating mainly downstream and the other with parabola-like crests not penetrating into an upstream wedge containing the second

quadrant. The parabola-like crests travel upstream with speeds greater than U while the crests of the other system shrink towards the downstream part of the forcing line. As $\sigma_0 \to 1$ the system with parabola-like crests gets compressed and disappears when $\sigma_0 = 1$, whereas the other system spreads out to propagate in all directions below a line through the forcing effect and perpendicular to the axis of rotation. For $\sigma_0 > 1$ there is only a single system of waves, propagating downstream in a wedge.

For each direction there is a particular frequency, namely $2\Omega \sin\alpha$, for which the forcing effect excites a 'column' which is composed of straight unattenuated waves of fixed frequency travelling (ahead and behind) parallel to the forcing line. Also there are two other systems, which propagate mainly downstream. The formation of the 'column' is very much similar to the formation of the 'Taylor column' even though their structures are quite different. But it is observed that the 'column' is the counterpart of the 'Taylor column' for an arbitrary α, for when $\alpha \to 0$ the 'column' and the associated wave systems do tend to the 'Taylor column' and cylindrical waves on the downstream side. The upstream 'column' is most prominent when $\alpha = 0$ and decreases as α increases, disappearing completely when $\alpha = \frac{1}{2}\pi$ while the downstream 'column' persists with some modifications.

In the steady case the disturbance is either found over the entire region below the line through the forcing effect and parallel to the axis of rotation or crosses it on the downstream side when $\alpha < 19°$. But if the forcing effect is oscillatory the disturbance penetrates into the region above this line both on the upstream as well as on the downstream side for all α. This is because in the steady case the longest waves always propagate parallel to the axis of rotation whereas a non-zero frequency makes it possible for them to propagate along directions inclined at $\pm \cot^{-1}(\sigma_0^{-2} - 1)^{\frac{1}{2}}$ to the axis of rotation. Unless α is very close to $\frac{1}{2}\pi$ there is always an influence on the upstream side. This upstream influence is to the left or to the right of the forcing line according as $\sigma_0 - \sin\alpha \lesseqgtr 0$ and increases as this quantity tends to zero. The caustic along the downstream part of the forcing line persists for all σ_0, leading to a concentration of wave crests along the downstream part of the forcing line.

The arbitrary inclination of the forcing line (not equal to zero or $\frac{1}{2}\pi$) makes the disturbed region asymmetric about the forcing line. When $\sin\alpha - \sigma_0 > 0$ the disturbed region to the left of the forcing line is always bigger than that on the right and the reverse situation occurs when $\sin\alpha - \sigma_0 < 0$. As α varies the wedges enveloping the possible wave systems rotate about the forcing effect in a direction opposite to that of the forcing line while the wave crests also undergo a kind of rotation about the caustic points with some minor modifications. The wave systems appearing for $0 < \sigma_0 < \sin\alpha$ are the counterparts of the wave systems excited by forcing effects travelling perpendicular to the axis of rotation for frequencies less than 2Ω. Similarly the wave systems appearing for $\sin\alpha < \sigma_0 < 1$ are the counterparts for $\sigma_0' < 2\Omega$ when the forcing effects travel parallel to the axis of rotation. Thus the arbitrary nature makes both kinds of wave system possible.

Once again from the analogy between the Boussinesq stratified fluid and the

homogeneous rotating fluid it follows that the wave pattern excited in a stratified fluid by a forcing effect travelling in a direction at $\frac{1}{2}\pi - \alpha$ to the vertical is similar to the mirror image in the forcing line of the pattern excited by a forcing effect travelling in a direction inclined at α to the axis of rotation. For this analogy to hold the forcing effects in both the fluid systems should be mirror images of each other in the forcing line, the other parameters being the same, 2Ω being replaced by N (the Brunt–Väisälä frequency). From the analogy it may be observed that the wave patterns described herein agree with that of Stevenson & Thomas (1969), who have studied both theoretically and experimentally the waves generated by a moving oscillating cylinder in a stratified fluid. For the 'column' case see their figures 6(*c*) and (*d*).

Part of this work was carried out while the author was a Junior Research Fellow of the Council of Scientific and Industrial Research, India, and the author is grateful for this financial help. The author also wishes to express his deep sense of gratitude to Professor Sir James Lighthill for the most helpful correspondence and for his elucidation of many aspects connected with this problem. Thanks are also due to Mr S. Sukavanam, who did much to improve the presentation of this paper, and to Professor S. D. Nigam and Dr V. Subba Rao for their interest and encouragement.

REFERENCES

Bretherton, F. P. 1967 *J. Fluid Mech.* **28**, 545.
Greenspan, H. P. 1968 *The Theory of Rotating Fluids.* Cambridge University Press.
Lighthill, M. J. 1960 *Phil. Trans. Roy. Soc.* A **252**, 397.
Lighthill, M. J. 1965 *J. Inst. Math. Applics.* **1**, 1.
Lighthill, M. J. 1967 *J. Fluid Mech.* **27**, 725.
Mowbray, D. E. & Rarity, B. S. H. 1967 *J. Fluid Mech.* **30**, 489.
Nigam, S. D. & Nigam, P. D. 1962 *Proc. Roy. Soc.* A **266**, 247.
Rarity, B. S. H. 1967 *J. Fluid Mech.* **30**, 329.
Stevenson, T. N. 1969 *J. Fluid Mech.* **35**, 219.
Stevenson, T. N. & Thomas, N. H. 1969 *J. Fluid Mech.* **36**, 505.
Subba Rao, V. & Prabhakara Rao, G. V. 1971 *J. Fluid Mech.* **46**, 447.
Veronis, G. 1970 *Ann. Rev. Fluid Mech.* **2**, 37.